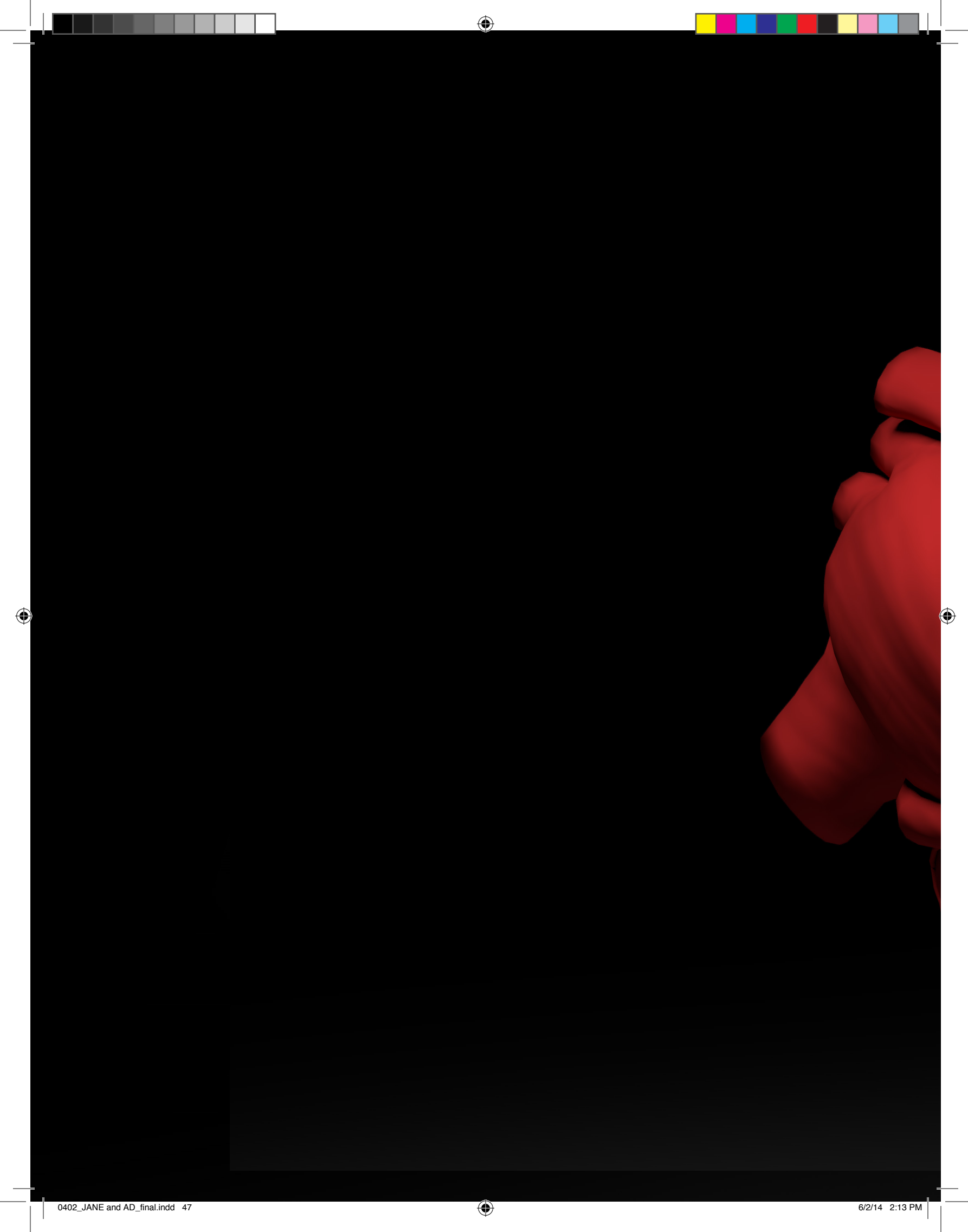


CURJ

**WINTER 2014
VOL. 15 NO. 1
CALTECH UNDERGRADUATE
RESEARCH JOURNAL**

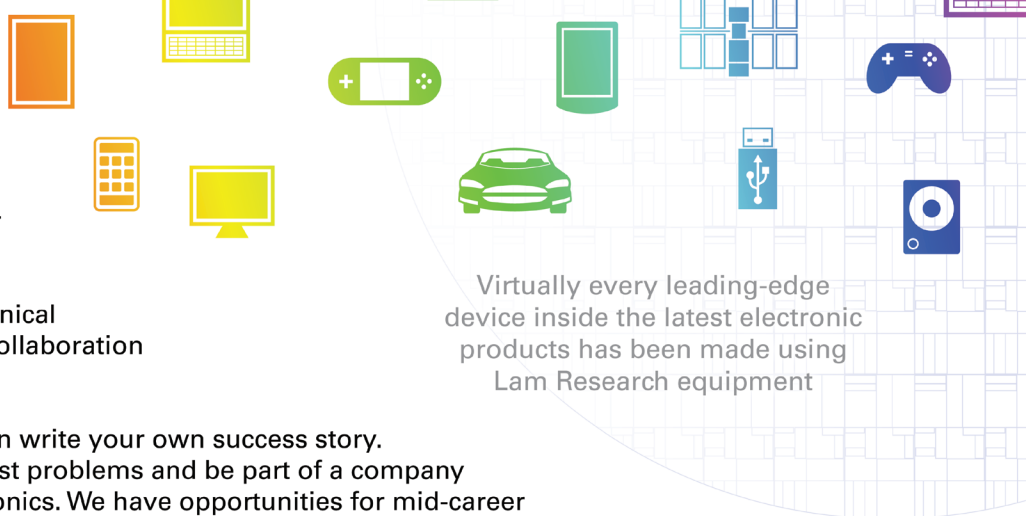




Now Hiring in North America, Asia, and Europe!

Success Starts Here

As a leading global supplier of wafer fabrication equipment and services to the semiconductor industry, Lam Research develops innovative solutions that help our customers build smaller, faster, and more power-efficient devices. This success is the result of our employees' diverse technical and business expertise, which fuels close collaboration and ongoing innovation.



Virtually every leading-edge device inside the latest electronic products has been made using Lam Research equipment

Join the Lam Research team, where you can write your own success story. Come help us solve our customers' toughest problems and be part of a company that plays a vital role in the future of electronics. We have opportunities for mid-career professionals and new college graduates (Ph.D., MBA, master's, and bachelor's). Lam Research has programs that allow individuals to continue their career development, build on their educational accomplishments, and play key roles in bringing innovative technology and business solutions to market in countries around the world.

Areas of opportunity:

- Business Development
- Chemistry (organic, inorganic)
- Engineering (chemical, computer, electrical, industrial, manufacturing and mechanical)
- Field Operations
- Finance
- Human Resources
- Information Systems
- Legal

Marketing/Communications

- Materials Science
- Operations/Supply Chain
- Physics
- Plasma Physics

Program and Project Management

- Quality
- Software Engineering

New College Graduates

Lam Research has programs that allow students to continue their career development and build on their educational accomplishments. We offer new college graduates the opportunity to play key roles in bringing innovative technology and business solutions to market in countries around the world.

College Internships

Lam's internship opportunities offer summer and/or co-op employment for students and provide hands-on business experience that complements academic studies. Students have the opportunity to work closely and learn from some of the best in the industry.

Experienced Professionals

If you are looking for a career in the highest of the high tech industries, join the company that takes you there – Lam Research Corporation. We are looking for the best and brightest to join our team of talented individuals.

For information about specific opportunities, please visit lamresearch.com/careers, where you can also apply online.

**Lam Research – a company where
successful people want to work**

lamresearch.com/careers

EOE/M/F/D/V



CURJ

Interview

5 Interview with Viviana Gradinaru

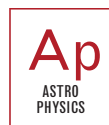
Research

9 Tissue Expansion for Organ Construction and
Tissue Regeneration



by Lisa Eshun-Wilson

17 Spin Alignment Effects in Black Hole Binaries



by Davide Gerosa

27 Research and Development of External Occulter
Technology for the Direct Observation of Extrasolar
Planetary Systems



by Herbert Franz Mehnert Stadelier

37 Developing Force Models for Full Body Contact and
Soft Tire-Solid Ground Interaction

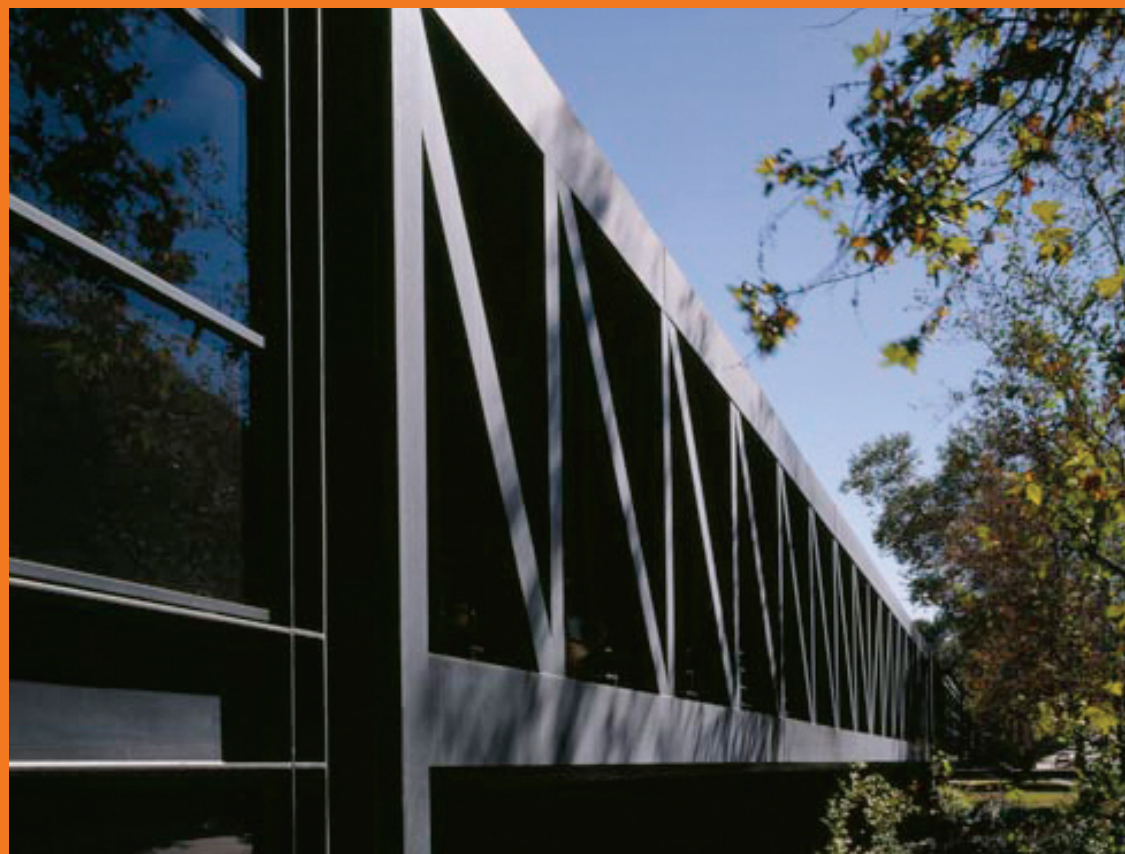


by Adam Ryason



Art Center College of Design

One of the world's preeminent art and design colleges, Art Center College of Design is renowned for its culture of innovation, rigorous transdisciplinary curriculum, superb professional faculty and extensive relationships with industry. For 80 years, Art Center has prepared an influential group of artists and designers to become leaders both in their chosen fields and the world at large.



UNDERGRADUATE PROGRAMS

- Advertising
- Entertainment Design
- Environmental Design
- Film
- Fine Art
- Graphic Design
- Illustration
- Photography and Imaging
- Product Design
- Transportation Design

GRADUATE PROGRAMS

- Art
- Broadcast Cinema
- Industrial Design
- Media Design



From the editors

EDITORS IN CHIEF

Edward Fouad
Conway Xu

ART DIRECTORS

Jane Park
Kevin Alexander
Murphy Armitage

CONTENT EDITORS

Edward Fouad
Suchita Nety
Jeff Shen
Shannon Wang
Caroline Yu

STAFF COLLABORATORS

Nils Lindstrom,
Art Center College of Design
Candace Rypisi,
Caltech Student-Faculty Programs
Susanne Hall,
Caltech Hixon Writing Center
Nareen Manoukian,
Caltech Hixon Writing Center
Charlyne Sarmiento,
Caltech Hixon Writing Center

CALTECH UNDERGRADUATE
RESEARCH JOURNAL vol. 15. no. 1

Welcome to the latest issue of the Caltech Undergraduate Research Journal! It is once again our pleasure to highlight some of the recent scientific accomplishments made by undergraduates at both Caltech and JPL. Summer after summer, talented and enthusiastic young scientists from around the world flock to Pasadena for 10 weeks to partake in numerous ongoing research projects led by our world-renowned scientists. These students have demonstrated a great commitment to science through their endeavors, and have helped contribute to the advancement of knowledge.

CURJ is honored to partner with all of Caltech's Student and Faculty Programs to highlight some of the cutting edge research done by four young scientists: Lisa Eshun-Wilson, Davide Gerosa, Herbert Mehnert, and Adam Ryason. Their research topics range from tissue regeneration to modeling tire-ground interactions, and the variety in their research showcases only a tiny portion of all the diverse research taking place at both Caltech and JPL.

With all the exciting student research at Caltech, let us not overlook the constant and unwavering support of the dedicated faculty and mentors. CURJ would like to thank all the faculty and mentors for their dedication and investment in the future of science. Moreover, CURJ is pleased to feature an interview of a new professor, Viviana Gradinaru, in this issue.

Professor Gradinaru is an expert in the field of optogenetics. She played an essential part in the development of optogenetics before arriving at Caltech. Since then, she has only further propelled this new field of biology. Currently, her lab at Caltech focuses on the neural connectivity in behavior and the development of tools for electrical and biochemical control of such neural connectivity. Fitting with the Caltech community's long history of scientists leading their fields, Professor Gradinaru is surely an inspiration to all young scientists.

Finally, we thank you for picking up this latest edition of CURJ and certainly hope that you enjoy it. As always, you can find more information about CURJ as well as previous issues on our website (curj.caltech.edu). Feel free to tell us your thoughts!

Best regards,




Edward Fouad and Conway Xu



Interview with Viviana Gradinaru



Viviana Gradinaru is an assistant professor at Caltech. She played an instrumental role in the development of optogenetics during her doctoral and postdoctoral studies at Stanford. Her lab is currently studying neural connectivity in behavior and developing tools for electrical and biochemical control. In the following interview, she discusses her research and road to academia, and offers advice to current students.

What are the big questions your lab is asking?

Our lab looks at the role that neuronal connectivity plays in behavior. We want to understand what underlies our behavior in different contexts and we think that the way that different neurons connect and communicate is the key to this. That's the big question. But to answer this question, we need tools to visualize and manipulate the neurons. Some of the existing tools are still inadequate, so we're working on new ones to activate and inhibit activity, as well as to map intact circuits. Optogenetics and CLARITY, which I worked on previously during my PhD and postdoc, are examples of these new tools. Of course, these are just starting points. If a project takes an interesting direction that we didn't anticipate, we'll follow it.

**What are some specific problems your lab is working on?**

We are interested in how much use and abuse our circuits can take before they malfunction. Aging is one factor we're looking at, and chronic stress is another. If you think about life at Caltech, it can be pretty intense and stressful! So how much stress can we take and even thrive with, and when is too much? What do circuits do when it's too much? Can we prevent or slow down the malfunctions in the brain?

Tell us about your work on Deep Brain Stimulation.

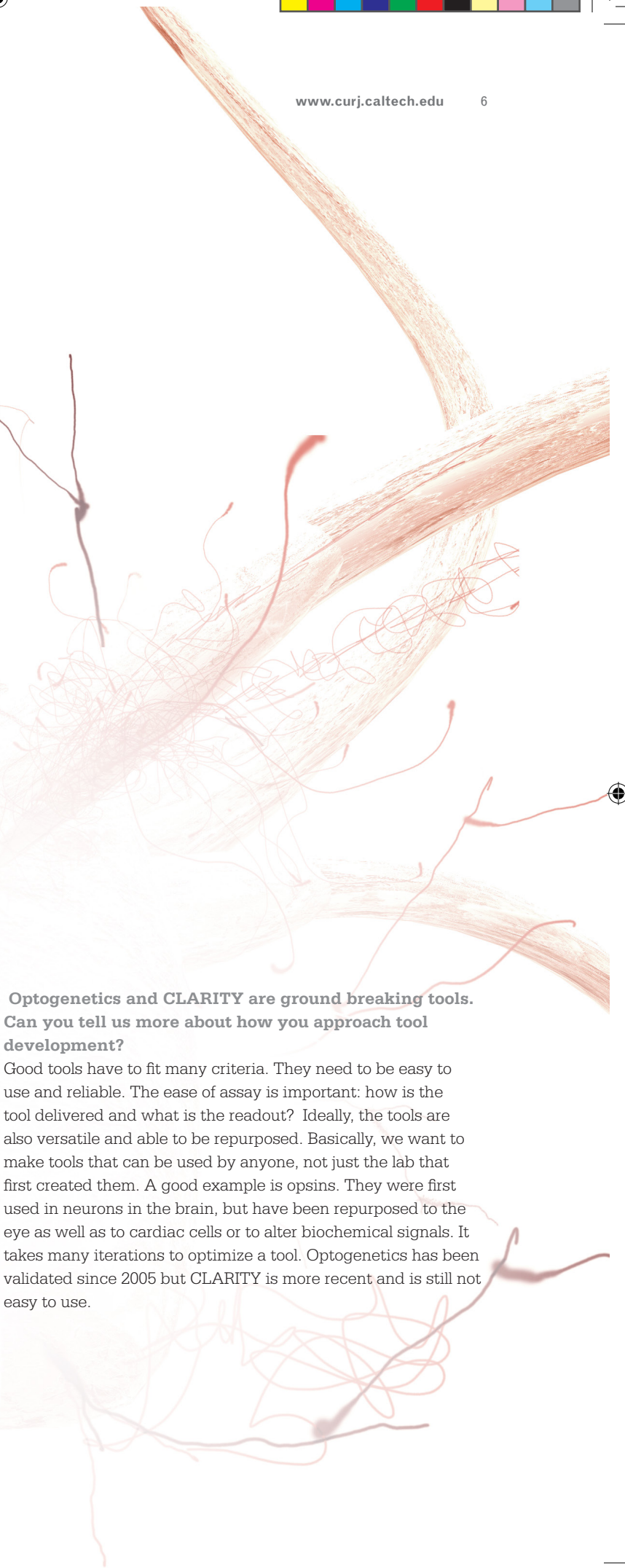
This ties into our research on aging, because a big problem with aging is Parkinson's disease. One current therapy for Parkinson's is deep brain stimulation, where you zap the brain in a particular spot and then the tremors go away. Surprisingly, the mechanism by which this works is still unknown. We want to know how DBS works, not only because of Parkinson's alone, but also for broader reasons: electrical stimulation of the brain can impact behavior. If we understand the mechanism, we can better predict which other circuits to target with DBS to aid in other disorders as well.

Do you foresee clinical uses of these tools?

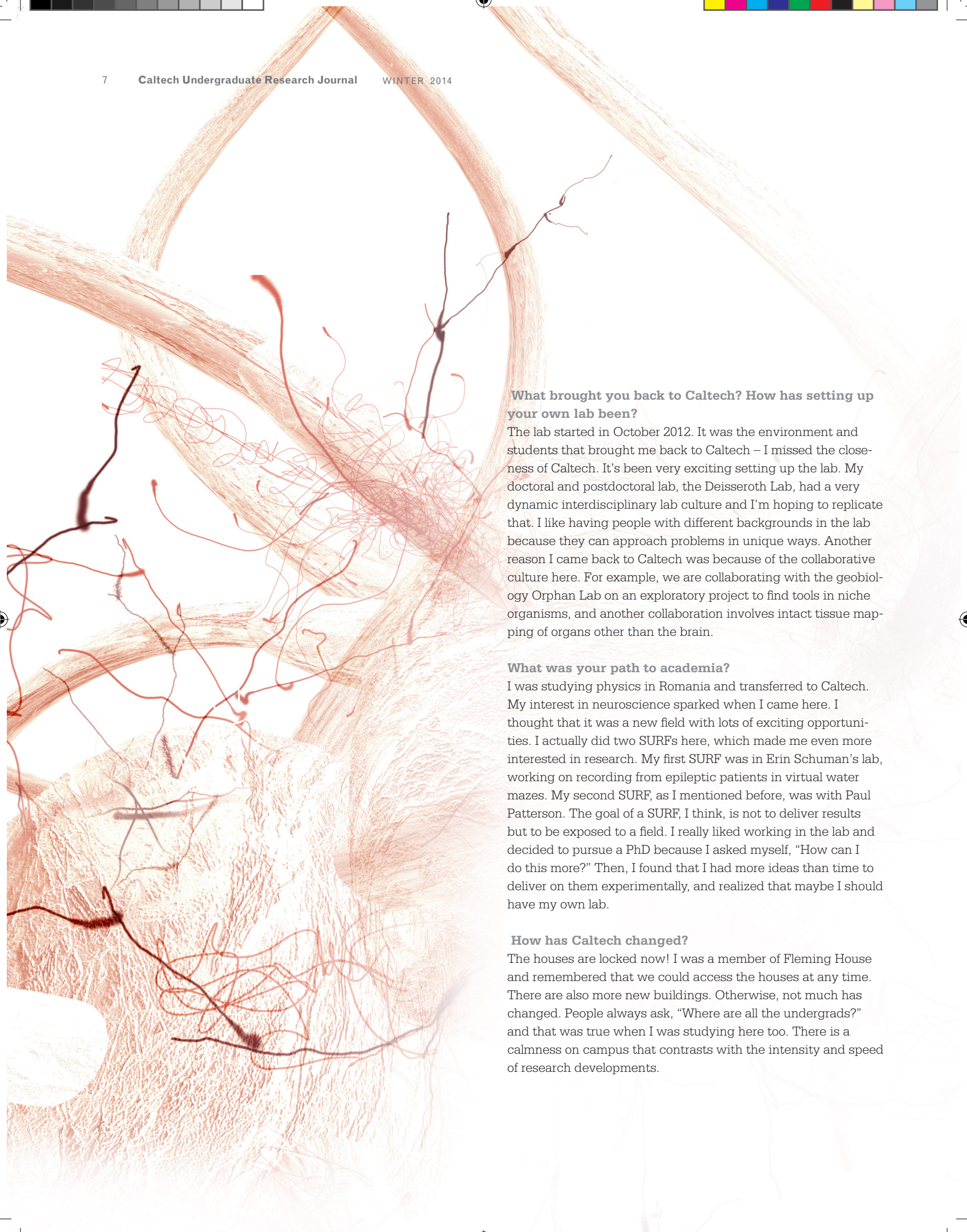
For researchers right now, these tools are allowing us to understand what circuits are responsible for the disease and for therapy. The field is still young and very much basic research at the moment, but I could imagine having optogenetic DBS or optogenetic rodent models for better drug screening.

What drew you to these types of questions?

The draw for neurodegeneration came from my research as an undergraduate here at Caltech. I was working with Paul Patterson on a project on Huntington's disease and we were introducing polyQ protein aggregates in culture. I learned a lot from this experience, but it emphasized to me the limited tools available to tackle intact systems.

**Optogenetics and CLARITY are ground breaking tools. Can you tell us more about how you approach tool development?**

Good tools have to fit many criteria. They need to be easy to use and reliable. The ease of assay is important: how is the tool delivered and what is the readout? Ideally, the tools are also versatile and able to be repurposed. Basically, we want to make tools that can be used by anyone, not just the lab that first created them. A good example is opsins. They were first used in neurons in the brain, but have been repurposed to the eye as well as to cardiac cells or to alter biochemical signals. It takes many iterations to optimize a tool. Optogenetics has been validated since 2005 but CLARITY is more recent and is still not easy to use.



What brought you back to Caltech? How has setting up your own lab been?

The lab started in October 2012. It was the environment and students that brought me back to Caltech – I missed the closeness of Caltech. It's been very exciting setting up the lab. My doctoral and postdoctoral lab, the Deisseroth Lab, had a very dynamic interdisciplinary lab culture and I'm hoping to replicate that. I like having people with different backgrounds in the lab because they can approach problems in unique ways. Another reason I came back to Caltech was because of the collaborative culture here. For example, we are collaborating with the geobiology Orphan Lab on an exploratory project to find tools in niche organisms, and another collaboration involves intact tissue mapping of organs other than the brain.

What was your path to academia?

I was studying physics in Romania and transferred to Caltech. My interest in neuroscience sparked when I came here. I thought that it was a new field with lots of exciting opportunities. I actually did two SURFs here, which made me even more interested in research. My first SURF was in Erin Schuman's lab, working on recording from epileptic patients in virtual water mazes. My second SURF, as I mentioned before, was with Paul Patterson. The goal of a SURF, I think, is not to deliver results but to be exposed to a field. I really liked working in the lab and decided to pursue a PhD because I asked myself, "How can I do this more?" Then, I found that I had more ideas than time to deliver on them experimentally, and realized that maybe I should have my own lab.

How has Caltech changed?

The houses are locked now! I was a member of Fleming House and remembered that we could access the houses at any time. There are also more new buildings. Otherwise, not much has changed. People always ask, "Where are all the undergrads?" and that was true when I was studying here too. There is a calmness on campus that contrasts with the intensity and speed of research developments.



The Alfred Mann Foundation is a nonprofit medical research

foundation, dedicated to bringing advanced medical technologies to the public to provide significant improvements to the health, security and quality of life for people suffering from debilitating medical conditions.

Feel free to visit our website: www.aemf.org, career section, from time to time to review our job openings.



Toyon's high caliber technical staff supports R&D efforts for the DoD.

We are looking for candidates with B.S., M.S. & Ph.D. degrees in engineering or the physical sciences. Opportunities exist in Santa Barbara, CA and Washington, DC.

- Radar & Optical Sensors
- Algorithm Development
- Modeling and Simulation
 - Systems Analysis

For career opportunities:
www.toyon.com

EOE M/F/D/V



TISSUE EXPANSION FOR ORGAN CONSTRUCTION AND TISSUE REGENERATION: A FOCUS ON DESIGN AND INSTRUMENTATION



Author: Lisa Eshun-Wilson
Hometown: Los Angeles, CA
College: Grinnell College
Major: Biochemistry with a concentration in Public Policy
Year: Class of 2014
Hobbies: Volunteering with kids; yoga; kickboxing
Mentors: Morteza Gharib and Hesham Azizgolshani
(Medical Engineering, California Institute of Technology)



A Growing Demand

The present need for transplant organs and soft tissue has exceeded the supply, and current research shows that this gap will continue to widen. Due to this demonstrated need, the field of tissue engineering has evolved to meet the demand. Tissue engineering, specifically, describes the interdisciplinary field involving the development of bioartificial implants and/or the art of tissue remodeling with the purpose of repairing or enhancing tissue or organ function. Interestingly, cell transplantation has been proposed as a potential alternative treatment to whole organ transplantation for failing or malfunctioning organs. This alternative may require only a very small number of donor cells to prepare the required implant because isolated cell populations can be expanded using *in vitro* cell culture techniques. Currently, to create an autologous implant, donor tissue is harvested and dissociated into individual cells for structural manipulation. The dissociated cells are attached and cultured onto a proper substrate that is ultimately implanted at the desired site of the functioning tissue. To properly conform to surrounding tissue, the implanted cells may require a material scaffold for structural support, which are based on synthetic extracellular matrices (ECMs), in the same way bridges require a strong foundation. However, there is a demand for tissue engineering methods that do not require scaffolds to reduce potential surgical complications.

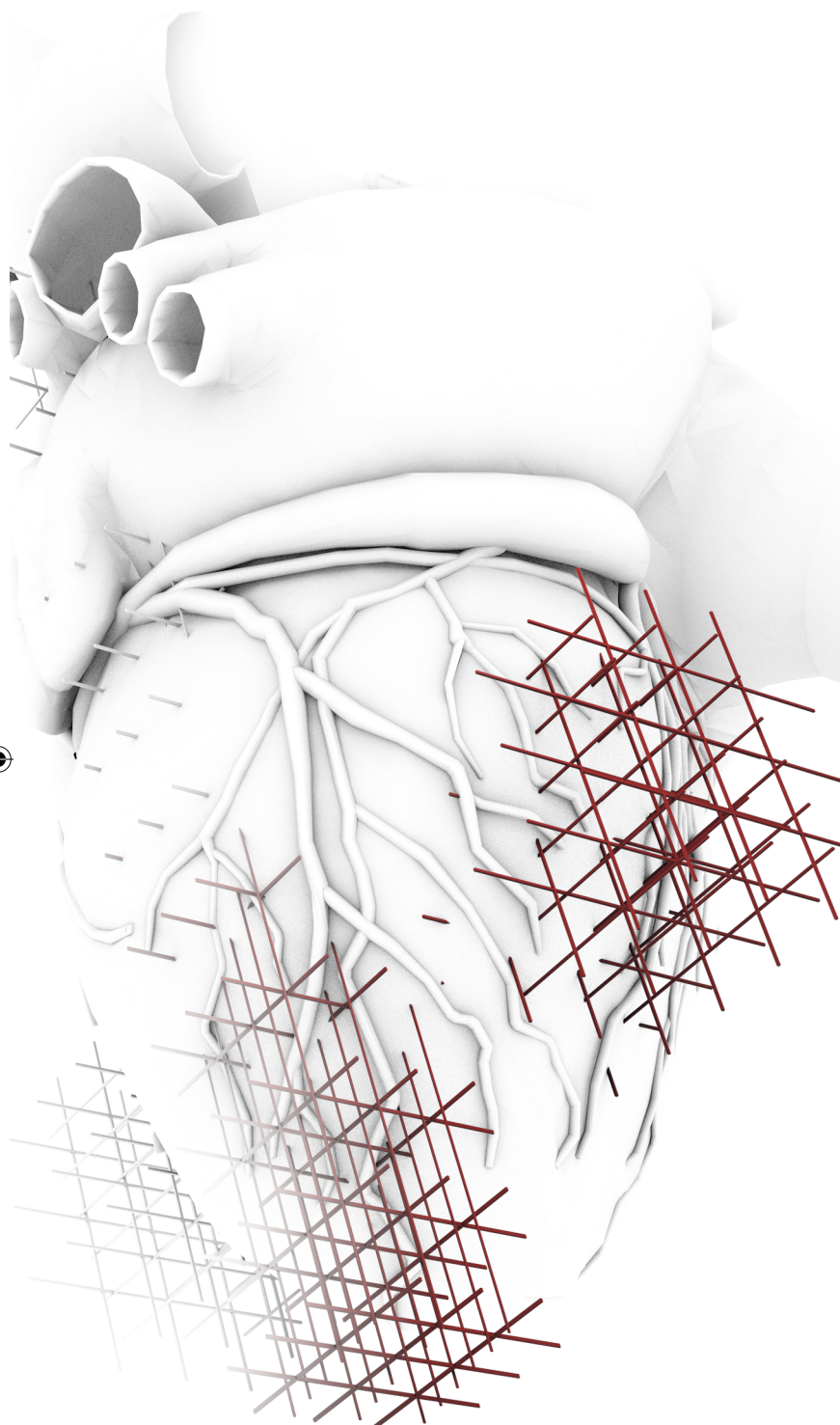
Successful applications of tissue regeneration procedures require a thorough understanding of the environment experienced by cells in normal tissues and by cells in bioartificial contexts before and after implantation. Thus, a better understanding of the cellular and molecular processes unique to living organisms and how to manipulate them is vital for combating the growing need for organs and tissue regeneration. Further, one of the major challenges of current biomedical research is to demystify not only the spatial organization of these complex systems, but also their spatiotemporal relationships. Studying the spatiotemporal relationships of cells will help us better understand cell and ECM interactions and how to provide structural support for tissue regeneration independently of material scaffolds. Our circulatory system serves an excellent example to illustrate this need. Given the pulsatile nature of blood flow, blood vessels are subjected to time-varying biomechanical forces in the form of stretch, such as cyclic mechanical strain, pulsatile pressure and shear stress. Luckily, the tunica adventitia, or

the outer most layer of the blood vessel, is comprised of connective tissue and works to regenerate lost or damaged tissue. The connective tissue responds to immediate biomechanical force signals through conserved response mechanisms, such as inflammation and tissue remodeling, which influence proliferation, cell migration, apoptosis, and cell and ECM interactions.

Cells that undergo mechanical stretch, or simulated biological stretch, have been found to proliferate at a higher rate due to the same effects. Fibroblasts serve as strong candidates in this experimental context because their biomechanotransduction pathways are highly stimulated by mechanical stretch. Fibroblasts are also major components of connective tissue and work to synthesize vital precursors of collagen and the extracellular matrix. In order to better understand the biomechanics at work here, past researchers have examined the effects of stretch and other forms of mechanical stress *in vitro* by culturing them on thin flexible substrates, or cell-viable plates, which are then mechanically deformed. However, little research has been done to examine the biomechanics of fibroblasts *in vitro* using rigid substrates.

The goal of this experiment was to examine the effect of mechanical stress on fibroblasts using time-lapse imaging to visualize cell proliferation induced by mechanically manipulated, cell-coated, rigid substrates. Time-lapse microscopy is a powerful technique used to image the same subject at regular time intervals over a period of time. Using this technique, one can observe the spatiotemporal relationships of the cell type of interest. However, in order to observe cell growth in a viable microenvironment, an incubator must be built around the microscope to sustain the biophysical needs of the cells. This study aspires to suspend NIH/3T3 fibroblasts between two rigid substrates, to simulate mechanical stimuli, and to generate new sheets of soft tissue *in vitro* and independently of a material scaffold. We hypothesized that as the distance between the substrates is increased, at the published proliferation rate of the NIH/3T3 cell line, the fibroblasts would populate the gap between the substrates and form monolayer sheets of fibroblasts (Fig. 1). The findings of the study consisted of the complete construction and configuration of the instrumentation required for the *in vitro* tissue expansion experiment.

“In the hopes of expanding soft tissue, the future steps of this study aim to utilize the newly configured instruments to generate sheets of fibroblasts that can be used in the place of material scaffolds for future tissue regeneration surgeries and organ generation experiments.”



The Research Process

In order to conduct an in vitro tissue expansion experiment, the instruments required for time-lapse imaging and to apply controlled mechanical stimuli, including the microscope incubation chamber and the micromanipulator were constructed and configured, respectively. First, the humidifier and incubation chamber evolved from the Kulesa and Kasemeier-Kulesa (2007) design to include laser-constructed acrylic hardware and allow for greater visualization techniques. Next, the heater system, composed of the single unit fan and the stainless steel finned heater, in addition to the stereomicroscope stage heater, brought the temperature in the chamber up to the optimal range at 36.5°C. The microprocessor based temperature controller was then wired to the heater and 100- Ω RTD probe. To meet additional atmospheric conditions for the cells, a CO₂ gas mixer was used to generate an approximate ratio of 5% CO₂ to Air with a flow rate of approximately 1 NL/min. The incubation chamber of 20" x 23" x 25" dimensions was found to hold 188 liters took 3.13 hours to reach optimal atmospheric condition.

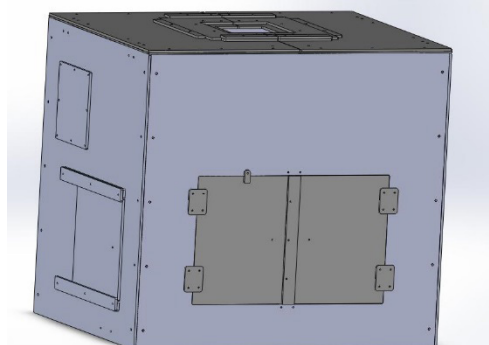
An incubator viability experiment was conducted to test how well the chamber grew the NIH/3T3 cell line for the in vitro tissue expansion experiment. The experiment showed that the NIH/3T3 cell line successfully grew within the atmospheric conditions of the incubation chamber when compared to the positive control, the Water Jacketed CO₂ Incubator (Table 1). At 12 hours, fibroblasts became 30-40% confluent within the incubation chamber and 50% confluent in the positive control (Table 1). At 24 hours, the previous adherent cell confluence rate was maintained, as expected for a dilution factor of 1:7 (Table 1). There were no signs of sustainable growth in the negative control, as expected (Table 1). To further explore the effect of mechanical strain on the fibroblasts, rigid substrates were chosen for the experiment. To test which substrate material would work effectively as an additional experiment, cells were grown on glass microscope slides with a dilution factor of 1:7 and monitored for 4 days. On day 4, there was successful growth of fibroblasts on the substrate. Further, the MT3-Z8 12 mm (0.47") motorized translational stages were configured using the Thorlabs APT software user interface in order to induce regulated levels of mechanical strain to the cells.



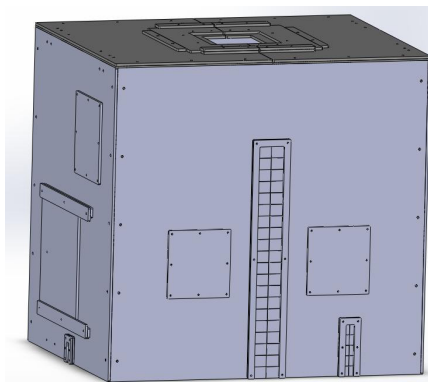
Be

www.curj.caltech.edu

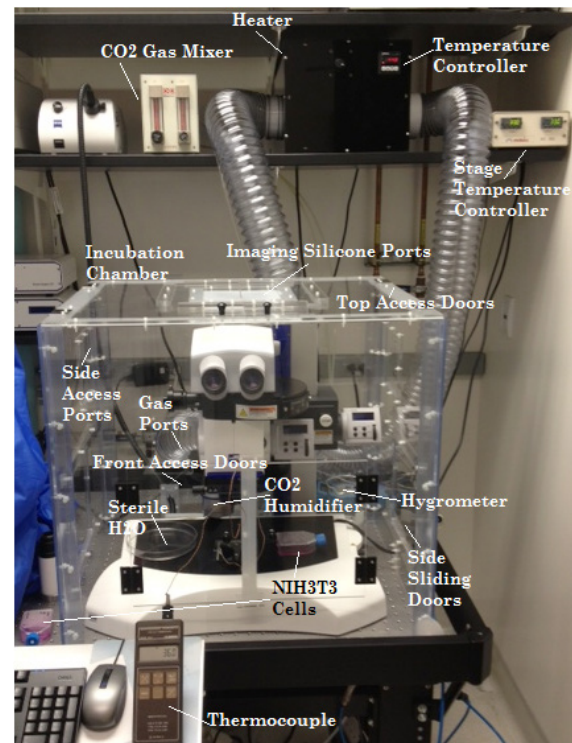
12



A.



B.



C.

Figure 1. Schematic view of the incubation chamber around stereomicroscope. (A) Front view of SolidWorks model of microscope incubation chamber. (B) Back view of SolidWorks model of microscope incubation chamber. (C) Photograph of the physically constructed incubation chamber. All interacting components are labeled in white.

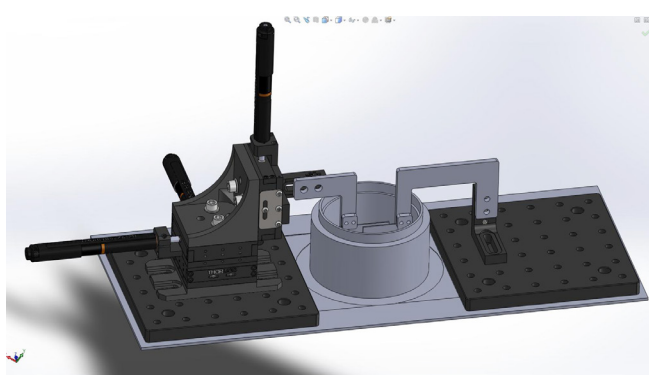


Figure 5. Screenshot of the Solidworks model of the micromanipulator, with its constructed arms and the bioreactor demonstrating how the mechanical stimuli would be applied. Both are placed on a simulated version of the microscope stage (in grey) to ensure that they will align with the dimensions of the incubation chamber.



What Does This Mean for the Future of Tissue Engineering?

The preliminary results of the incubator viability experiment showed that NIH/3T3 cells were able to successfully proliferate under the administered atmospheric conditions. The initial incubator design was very similar to that of Kulesa and Kasemeier-Kulesa (2007), but the final design included different materials and prioritized different operational methods. The final design featured access ports, sliding doors, gas ports, an imaging port, and silicone gaskets that enhanced user experience, maintained the required environmental conditions, and accommodated the moving parts of the stereomicroscope. The combined effect of the newly constructed heater and the microscope stage heater led the temperature to stabilize at 36.5°C and the humidity to reach 42%. The humidity was reasonably low in comparison to the CO₂ Water Jacketed Incubator at approximately 63% and this may have inhibited the cells from reaching their optimal growth rate and cell size. Additionally, cells grown under the conditions of the positive control were more analogous to the anticipated spindle-like shape for fibroblasts, while cells grown in the incubation chamber did not branch out as drastically.

Current findings assert that cultured fibroblasts possess a characteristic polarized phenotype manifested by an elongate cell body with an anterior lamella whose cell edge is divided into protrusion-forming and inactive zones, which can impact cell-cell interactions (Gelfand 2002). So it is imperative that the humidity is raised to produce cells with the optimal cell shape for effective cell signaling activity in the in vitro tissue expansion experiment. Specifically, NIH/3T3 cells are significantly sensitive to contact inhibition. This characteristic may affect the fibroblast proliferation rate and their ability to form sheets (Holly and Kiernan 1968). Increasing the internal humidity levels will facilitate optimal cell shape and therefore better cell-cell intracellular signaling. Our study highlights a primary challenge in the field of tissue engineering for tissue expansion in vitro experiments: replicating a viable microenvironment for the cells. In the hopes of expanding soft tissue, the future steps of this study aim to utilize the newly configured instruments to generate sheets of fibroblasts that can be used in the place of material scaffolds for future tissue regeneration surgeries and organ generation experiments. Societal implications include reducing surgical invasiveness in current tissue regeneration methods and providing a stepping-stone for successful organ construction.

Future Directions

As a future experiment, the humidifier can be optimized to achieve a higher humidity percentage. Currently, a 250 mL Erlenmeyer flask is being used as the water reservoir for the humidifier. This size could be increased to improve gas flow from the CO₂ glass bubbler to the incubation chamber. In addition to optimizing the humidifier, the CO₂ levels may require a microprocessor based CO₂ sensor to be verified. Currently, the gas mixer is calibrated to maintain a 5% ratio of CO₂ to air; however, future steps can include acquiring a CO₂ sensor to confirm the ratio because gas leakage may occur and affect CO₂ levels. This study also showed that the NIH/3T3 cell line could effectively grow on rigid substrates. Preliminary results from the glass substrate experiment demonstrate that cells can grow on plain, non-treated glass microscope slides in 100 mm petri dishes. Therefore, the glass microscope slides may serve as the rigid substrates in the in vitro tissue expansion experiment.

Further, future investigations can explore how treated glass substrates compare to non-treated substrates and also how different materials affect cell proliferation; for example, polystyrene versus glass microscope slides. Another key experiment that can optimize the conditions for the in vitro tissue expansion experiment include growing cells on two separate substrates and examining how the cells transfer from one platform to the next. The Gharib Research Group has successfully conducted this experiment before, but future steps include experimenting with new materials for optimal transfer. This will help determine whether both substrates will need to be cell-coated, as the two substrates are incrementally pulled apart by the micromanipulator.

As a result this study's findings, the software installation process and initial configuration for the micromanipulator was completed by our research team. Additionally, the arms that the micromanipulator will use to apply controlled levels of mechanical strain to generate sheets of fibroblasts at the rate of the published value of the NIH3T3 cell proliferation rate have been constructed and are ready for manually assembly. The bioreactor design has been finalized and is also ready to be manufactured and assembled inside the incubation chamber. Future research to improve the design of the bioreactor can work to ensure that the arms of the micromanipulator can efficiently access the substrates suspended



within the growth media of the bioreactor on the stage of the stereomicroscope. Upon the final assembly, the micromanipulator sequence can be edited to dictate the levels of mechanical strain and the length of the fibroblast sheet. Key characteristics of the fibroblasts can be more closely examined, including collagen synthesis, extracellular matrix synthesis, and/or migratory behaviors, based on which variables are deemed appropriate. We hope that these further analyses will take us one step closer to successfully generating sheets of soft tissue for effective manipulation and thus meet the demand to reduce the use of material scaffolds in order to diminish the risks and surgical complications associated with their use today.

"The preliminary results of the incubator viability experiment showed that NIH/3T3 cells were able to successfully proliferate under the administered atmospheric conditions."

	Positive Control	Experimental Variable	Negative Control
0 hours			
12 hours			
24 hours			

Table 1. Results of the Incubator Viability Test. 3 T-25 flasks were prepared with the NIH/3T3 cell line and grown at the positive control site, negative control site, and the experimental site. The incubation chamber performance was compared to that of the Water Jacketed CO₂ Incubator. Pictures were taken using the IPX-VGA210-G IMPERX camera and obtained for analysis using the LYNX GigE software. Cells were observed at 3 time points [0 hours, 12, hours, and 24 hours].

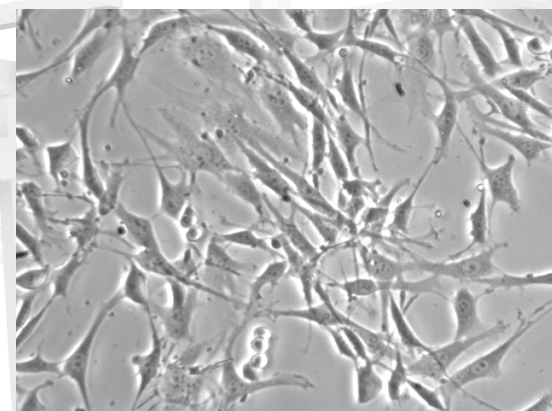


Figure 2. Results of the substrate adherence test. Cells were grown on clear microscope slides in 100 mm petri dishes in 1X Dulbecco's Modified Eagle's Medium/10% Fetal Bovine Serum/1% Streptomycin-Penicillin with a dilution factor of 1:7. Picture was taken 96 hours following incubation time with the IPX-VGA210-G IMPERX camera and obtained for analysis using the LYNX GigE software.



Further Reading

Cohen, S., Bano, M.C., Cima, L.G., et al. 1993. Design of synthetic polymeric structures for cell transplantation and tissue engineering. *Clin. Mater.* 13: 3.

Kulesa, P. M., and J.C. Kasemeier-Kulesa. 2007. Construction of a Heated Incubation Chamber around a Microscope Stage for Time-Lapse Imaging. *Cold Spring Harbor Protocols* 14: doi:10.1101/pdb.prot

Lehoux, S. and A. Tedgui. 2003. Cellular mechanics and gene expression in blood vessels. *Journal of Biomechanics* 36: 631-643

Yang, Shoufeng, Kah-Fai Leong, Zhaohui Du, and Chee-Kai Chua. 2001. The Design of Scaffolds for Use in Tissue Engineering. Part I. Traditional Factors. *Tissue Engineering* 7: 679-689

Acknowledgements

I would like to thank the Gharib Research Group and the Option of Medical Engineering for their commitment, resources, and guidance. Thank you to Howard Hughes Medical Institute for funding my amazing experience. And special thank you to my mentors Vice Provost Morteza Gharib, Ph.D. and Hesham Azizgolshani, Ph.D., as well as the Student-Faculty Programs office of the California Institute of Technology for making this amazing opportunity a possibility for me.



**INNOVATORS
WANTED**

At Curtiss-Wright, innovators like you can develop the next generation of technology for tomorrow's most advanced defense and aerospace platforms.

We are the largest supplier of rugged, embedded computing modules and subsystems for air, ground and sea platforms. And we've been doing it for more than 80 years.

Consider a career in a rewarding, fast-paced environment where you will work with some of the most talented engineers in the defense industry.

**CURTISS -
WRIGHT**

Visit our careers page at: <http://www.cwcdefense.com/careers.html>
Send your resume to: hiring@curtisswright.com



AFRL
THE AIR FORCE RESEARCH LABORATORY
LEAD | DISCOVER | DEVELOP | DELIVER

IMAGINE THE IMPOSSIBLE
POSSIBLE

A FEW DIVERSITY COMPANY
Chosen By
The Readers Of
Diversity/Careers
2012

Come join the Air Force Research Laboratory (AFRL) team where diversity in talent, background, ideas and beliefs allows us to create tomorrow's technologies today...



www.TeamAFRL.com  www.USAJOBS.gov

AFRL offers civilian career opportunities in engineering, math, science and medical disciplines.



Author: Davide Gerosa
Hometown: Monza, Italy
College: Università degli Studi di Milano (University of Milan, Italy)
Major: Physics
Year: Class of 2013
Hobbies: Rock music, skiing, mountain climbing
Mentors: Emanuele Berti (California Institute of Technology and University of Mississippi) and Yanbei Chen (California Institute of Technology)



Spin Alignment Effects in Black Hole Binaries



Black holes (BH) are regions of space-time with gravity so intense it prevents everything, even light, from escaping. Surprisingly, BHs are very simple objects, characterized by only two parameters: their mass M and their angular momentum, or spin, χ . Observations suggest that BHs exist only in two well separated mass ranges: smaller stellar-mass black holes with $M \sim 10M_\odot$ and supermassive black holes with $M \sim 10^6 - 10^{10} M_\odot$. Stellar-mass BHs result from the gravitational collapse of the most massive stars when they explode as Supernovae. On the other hand, super-massive BHs are hosted by galaxies in central bulges that grow due to accretion and repeated merging events. In both mass ranges, BHs can form binary systems. If the separation between the two BHs is small enough, the evolution of the binary is ruled by gravitational-wave (GW) emission that carries energy away from the system, leading to a merging event. At wider separation, the evolution is dominated by interactions with the astrophysical environment, such as accretion disks in the supermassive case and nearby stars for stellar-mass binaries. This phase can alter the BH parameters: mass, spin magnitude and spin orientation. Spin-alignment in stellar-mass BH binaries will be the main topic of this paper.

Stellar-mass BHs are extremely important in astronomy, because they are thought to be one of the evolutionary endpoints for massive stars, and the collapse of their progenitor stars enriches the Universe with heavy elements. Since neutron stars cannot be more massive than about $3M_\odot$, mass measurements of compact objects above this limit are indirect observations of BHs. Today ~ 50 systems are known to host a compact object too massive to be a neutron star. However, this is just a small sample of a total number of $\sim 10^8$ to 10^9 stellar-mass BHs that are believed to exist in the Milky Way.



Our main motivation for studying spin alignment of stellar-mass black-hole binaries is the imminent birth of GW astronomy, which can potentially directly detect BH presence.

Our main motivation for studying spin alignment of stellar-mass black-hole binaries is the imminent birth of GW astronomy, which can potentially directly detect BH presence. GWs are ripples of curvature in the space-time produced by the motion of massive bodies. Unlike X-rays, which emit from the material accreting onto the BH, not the BH itself, GW signals are directly emitted from BHs. This is therefore an unambiguous method to determine the nature of a BH. The direct detection of GWs is experimentally challenging, and has yet to come, but with the ongoing installation and commissioning of the Advanced LIGO and Advanced Virgo detectors, direct discovery of GWs may happen in the next few years. Gravitational-wave signals need to be extracted from noisy data using matched filtering, which consists of computing the cross-correlation between the output coming from the detector and a predicted theoretical waveform, or template. Detection rates increase by a factor ~ 30 to ~ 100 if matched filtering is used, but a detailed knowledge of the incoming waveform is required. It is therefore critical to model the dynamics of possible GW sources.

The life of a compact binary as GW source can be divided into three main stages, each of them producing a different GW signal: inspiral, merger and ringdown. During the inspiral phase the orbit of the binary decreases due to the emission of gravitational radiation that carries energy away from the system. The separation can decrease until the BHs merge with each other into a more massive BH. The merger remnant is a highly distorted BH that approaches its final equilibrium configuration by emitting gravitational waves of characteristic frequency and damping time: this is known as the ringdown phase.

Since sources become detectable during the inspiral phase, it is critical to predict the binary dynamics (including the spin orientations) with accurate precision in this phase. The inspiral phase of a compact binary is studied using three different approaches. At high separation, the stars come together due to interactions between them and with the astrophysical environment. At smaller separation, the dynamics of the binary decouple from the environment and the inspiral is described by General Relativity with space-time curved by the presence of the BHs. Between these two regimes, where the evolution is dominated by GW emission but the general relativistic effects are weak, the evolution can be studied using the Post-Newtonian approximation, i.e. expanding the Einstein equations of General Relativity in a series of v/c (where v is the orbital velocity and c is the speed of light) and considering just the leading-order terms.

During the post-Newtonian inspiral, BH binaries can pass through coplanar equilibrium solutions of the post-Newtonian equations and remain locked in these resonant configurations. The presence of such resonances is a natural physical mechanism to cluster samples of binaries with well defined spin orientations: both the spins and the orbital angular momentum tend to lie in the same plane just before merger. The effect of resonances strongly depends on the initial conditions of the post-Newtonian inspiral, i.e. on the formation history of the binary. Ultimately, our goal is to understand if the existence of post-Newtonian resonances can simplify the construction of matched-filtering templates in binary BH data analysis.



Ultimately, our goal is to understand if the existence of post-Newtonian resonances can simplify the construction of matched-filtering templates in binary BH data analysis."

Spin Orbit Resonances

We performed post-Newtonian simulations of statistical samples of binaries starting from a separation $R = 1000M$ to $R = 10M$ (hereafter we use geometrical units $G = c = 1$). The equations of motion depend on ten variables: the spins S_1 and S_2 , the direction of the orbital angular momentum L and the orbital velocity parameter v . There are also 3 constraints (at the post-Newtonian order we consider): the spin magnitudes are constant and L is a unit vector, so there are seven degrees of freedom. As reported in Fig. 1, we choose a system of reference with the z -axis oriented along L , and we define θ_1 and θ_2 to be angles between the two spins and orbital angular momentum ($\cos \theta_i = S_i \cdot L$), and we denote $\Delta\Phi$ as the angle between the projections of the spins on the orbital plane. The masses of the two BHs m_1 and m_2 are often combined using $M = m_1 + m_2$ (total mass) and $q = m_2/m_1$ (mass ratio), and the spins are typically indicated using $0 < \chi_i = S_i/m_i^2 < 1$. The full set of equations used in this project is reported in our further study where citations are also given for each of the various terms implemented. The post-Newtonian equations for the spin evolution are typical precession equations. The angular momentum is conserved on the precessional timescale, and the energy of the system decreases over the (longer) radiation reaction timescale due to GW emission.

Resonant configurations are families of equilibrium solutions in which the two BH spins and the orbital angular momentum are coplanar, precessing jointly about the total angular momentum. For a fixed value of the orbital angular momentum, i.e. at a particular point in time during the inspiral, the resonant configurations can be found by forcing the three vector S_1 , S_2 and L to lie in a plane ($\Delta\Phi = 0, \pi$) and solving for those values of θ_1 and θ_2 which satisfy the post-Newtonian equation of motion. Solutions for the $\Delta\Phi = 0$

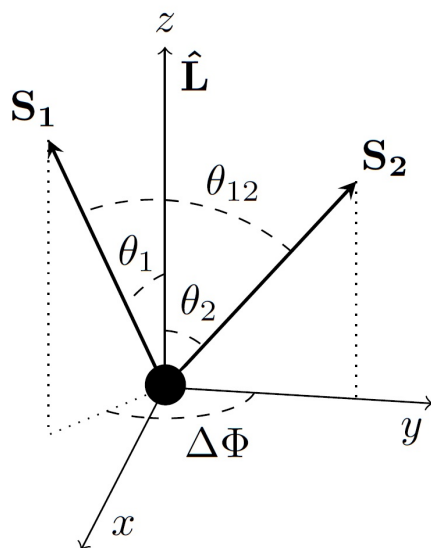


FIG. 1. Reference system adopted to describe the post-Newtonian inspiral. The three independent variables in the post-Newtonian evolution are the angles between the spins and the orbital angular momentum θ_1 and θ_2 , and the angle between the projection of the spins on the orbital plane $\Delta\Phi$. We also define θ_{12} to be the angle between the two spins.

configuration can be found if $\theta_1 < \theta_2$, while the $\Delta\Phi = \pi$ resonance affects just those binaries with $\theta_1 > \theta_2$. As the separation decreases due to the emission of GWs, the resonant values of θ_1 and θ_2 change, spanning a big region in the (θ_1, θ_2) parameter space: in particular, the solutions evolve toward configurations with $\theta_1 = \theta_2$. If the binary crosses one of these resonant configurations during the inspiral phase, the system can remain locked into it. Once the system is locked there is no free precession anymore, but the evolution continues oscillating around a resonant configuration.

To show these resonant effects we ran a Monte-Carlo simulation evolving a sample of 1000 BH binaries with $q = 9/11$ and $\chi_1 = \chi_2 = 1$ from $R = 1000M$ to $R = 10M$, when non-linear effects become stronger and the post-Newtonian approximation fails. As initial conditions, we chose a uniform distribution of $\cos\theta_1$, $\cos\theta_2$, and $\Delta\Phi$. In Fig. 2, we show different snapshots of the evolution: to stress the role of the two different resonances, the binaries are colored with respect to their initial value of θ_1 and θ_2 . In the top-left panel of Fig. 2 we show the evolution in the $(\cos\theta_1, \cos\theta_2)$ plane: the binaries evolve along lines over which the projection $S_0 \cdot L$ is approximately constant, where S_0 is defined to be: $S_0 = (1+q)S_1 + (1+q-1)S_2$.

The locking into resonance is evident in the top-right panel of Fig. 2, where the evolution is shown in the $(\Delta\Phi, \cos\theta_{12})$ plane, with $\cos\theta_{12} = S_1 \cdot S_2$. The presence of such resonant configurations causes a clear segregation of the sample. If the more massive black hole is more aligned with the orbital angular momentum than the less massive one ($\theta_1 < \theta_2$, red points) the evolution is strongly influenced by the $\Delta\Phi = 0$ resonance and it will generally align the two spins with each other ($\cos\theta_{12} \rightarrow 1$); if instead the less massive BH is initially more aligned ($\theta_1 > \theta_2$, blue points), then the $\Delta\Phi = \pi$ resonance forces the spins of the locked binaries to be anti-aligned with each other ($\cos\theta_{12} \rightarrow -1$). These results are still valid but less evident for isotropic samples with lower values of q and χ_i . In the bottom panels of Fig. 2 we show the evolution of an isotropic sample of BH binaries with $q = 1/3$ and $\chi_1 = \chi_2 = 1$.

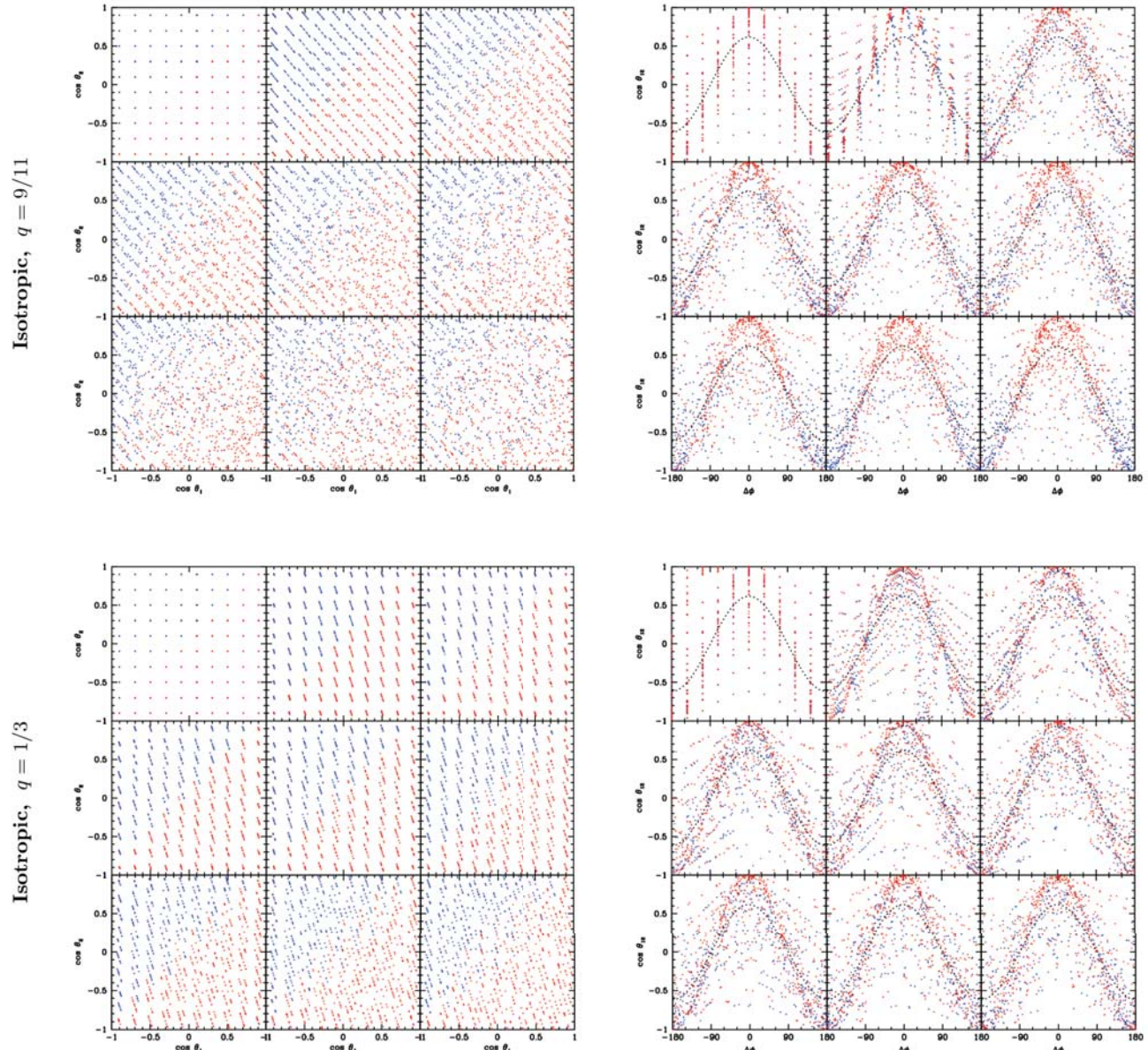


FIG. 2. Distribution of $(\cos \theta_1, \cos \theta_2)$, left panels, and of $\Delta\Phi, \cos \theta_{12}$, right panels for an isotropic sample of maximally spinning BH binaries with $q = 9/11$, top panels and $q = 1/3$, bottom panels. In each panel the evolution is plotted for different separations: from right to left and from top to bottom, at $R = 1000M$ (initial conditions), $R = 1000M$ (slightly after the beginning of the post-Newtonian evolution), $R = 750M$, $R = 500M$, $R = 250M$, $R = 100M$, $R = 50M$, $R = 20M$, $R = 10M$. Red points start with $\cos \theta_1 > \cos \theta_2$, blue points start with $\cos \theta_1 < \cos \theta_2$; the black dotted line is the expected correlation between $\cos \theta_{12}$ and $\Delta\Phi$. The region of influence of each resonance is stressed: red binaries tend to cluster about $\Delta\Phi = 0^\circ$ while blue binaries are attracted by $\Delta\Phi = 180^\circ$.



Ap

www.curj.caltech.edu 22



We presented a set of phenomenological models exploring the different possibilities predicted by BH-binary formation models. The simulations presented here show a critical dependence on the spin-orbit resonant locking on the statistical (a)symmetry of the initial conditions.



Astrophysically-motivated Initial Condition

The key element to predict the spin orientation is a proper initialization of the direction of the spins that results from previous interaction with the astrophysical environment (at $R > 1000M$). Each binary star has to undergo two supernova events to become a BH binary: each explosion imparts a kick to the newly formed BH. Before the explosions, the spin axes of both stars in the binary are parallel to the orbital angular momentum. The inclination between the BH spins and the orbital plane is natal in nature, i.e. it comes from the asymmetry of the supernova explosion itself. The kick coming from the explosion changes both direction and magnitude of the velocity of the newly formed BH around the companion, modifying the direction of the orbital plane but leaving the spins parallel to each other. If the binary remains bound, the system will be in a configuration with both spins misaligned by the same angle with respect to the orbital angular momentum ($\theta_1 \sim \theta_2$). Another possibility is that between the two explosions, when the system contains a star and a BH, the spin of the BH can be realigned by mass transfer and tidal interaction from the companion. If this alignment happens, after the second explosion the system would be in a configuration with one spin nearly aligned with the orbital angular momentum, and the other misaligned as in the previous case. The post-Newtonian resonant configurations were not studied under these initial conditions, and they can deeply modify the spin orientations before the merger.

5.





We developed three phenomenological models, in which (i) both BH are misaligned, (ii) only the primary or (iii) the secondary is misaligned. We keep the mass ratio and the spin magnitudes fixed to $q = 9/11$ and $\chi_1 = \chi_2 = 1$. We also keep the main misalignment fixed to 10° with a dispersion of 3° . These numbers are inspired by previous population-synthesis studies and they should be taken as illustrative of the qualitative effects of resonances in these formation scenarios. We always choose $\Delta\Phi$ uniformly in $[-\pi, \pi]$ because $\Delta\Phi$ is the initial phase of the precession. Our configurations are:

- (10-10): both spins are misaligned by the same angle with respect to the orbital angular momentum: θ_1 and θ_2 are uniformly drawn in cosine in the range $[10^\circ - 3^\circ, 10^\circ + 3^\circ]$;
- (10-0): secondary BH realigned by mass transfer events: θ_1 is uniformly drawn in cosine in the range $[10^\circ - 3^\circ, 10^\circ + 3^\circ]$ and θ_2 in $[0^\circ, 3^\circ]$;
- (0-10): primary BH realigned by mass transfer events: θ_1 is uniformly drawn in cosine in the range $[0^\circ, 3^\circ]$ and θ_2 in $[10^\circ - 3^\circ, 10^\circ + 3^\circ]$.

Fig. 3 shows snapshots of the post-Newtonian evolution with the same conventions of the previous figures for each different run. In the (10-10) run, there is no efficient locking in the post-Newtonian resonances. Even at very late times ($R \sim 10M$), binaries remain scattered through all the available range in $\Delta\Phi$. The number of binaries that precess freely is always bigger than the number of binaries locked in a resonant configuration. The resonances still exist, and remain solutions of the post-Newtonian equations, but their effect is statistically insignificant. On the other hand, the locking is extremely efficient in both the (10-0) and the (0-10) runs: almost all binaries are locked around $\Delta\Phi = 0$ or $\Delta\Phi = \pi$. The samples are almost perfectly segregated by the post-Newtonian evolutions.

The resonant locking is evident only if the initial angles θ_1 and θ_2 are different from each other. Our results show that the relative spin alignment at the beginning of the simulation is crucial to determine whether binaries will lock into resonance. Mass transfer events, tidal interactions and the subsequent alignment of the first-born BH are crucial to predict the spin parameters at the end of the inspiral, just before the merger.

In this work we presented a set of phenomenological models exploring the different possibilities predicted by BH-binary formation models. The simulations presented here show a critical dependence on the spin-orbit resonant locking on the statistical (a)symmetry of the initial conditions. We further improved our astrophysical assumption in a dedicated paper, to which we refer for interested readers.

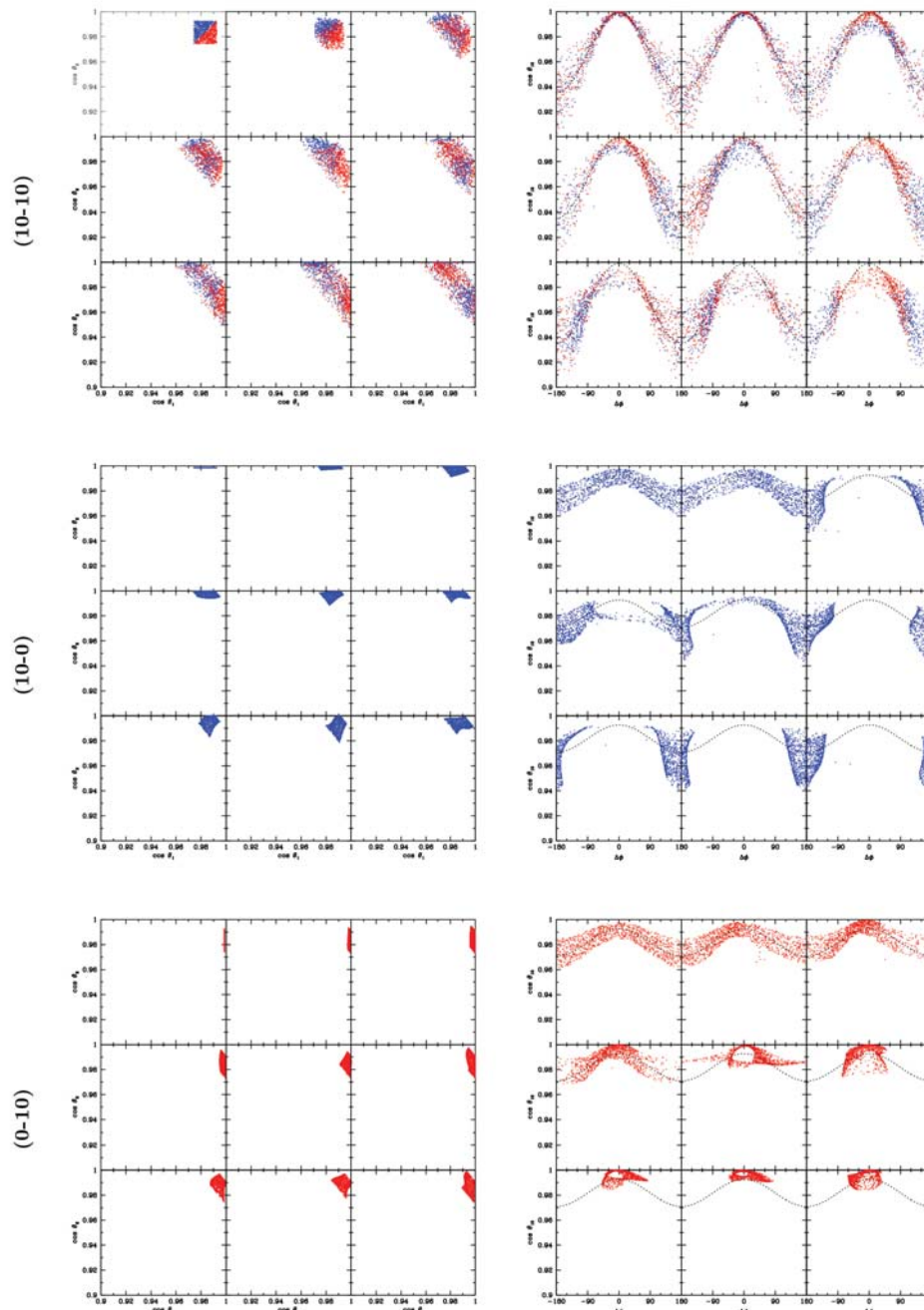


FIG. 3. Distribution of $(\cos \theta_1, \cos \theta_2)$, left panels, and of $(\Delta\Phi, \cos \theta_{12})$, right panels for our three astrophysically motivated samples of maximally spinning BH binaries with $q = 9/11$: (10-10), (10-0) and (0-10). In each panel the evolution is plotted for different separations: from right to left and from top to bottom, at $R = 1000M$ (initial conditions), $R = 1000M$ (slightly after the beginning of the post-Newtonian evolution), $R = 750M$, $R = 500M$, $R = 250M$, $R = 100M$, $R = 50M$, $R = 20M$, $R = 10M$. Red points start with $\cos \theta_1 > \cos \theta_2$, blue points start with $\cos \theta_1 < \cos \theta_2$; the black dotted line is the expected correlation between $\cos \theta_{12}$ and $\Delta\Phi$. For both the (10-0) and the (0-10) run, the width of the $\Delta\Phi$ distribution clearly decreases during the inspiral, because of the strong resonant locking. The effect is absent in the (10-10) run where binaries freely precess even down to $R = 10M$.



Further Reading

- 1. D. Gerosa, M. Kesden, E. Berti, R. O’Shaughnessy, and U. Sperhake. Resonant-plane locking and spin alignment in stellar-mass black-hole binaries: A diagnostic of compact-binary formation. *Phys. Rev. D* 87, 104028 (2013).
- 2. B. S. Sathyaprakash and B. F. Schutz. Physics, Astrophysics and Cosmology with Gravitational Waves. *Living Reviews in Relativity* 12, 2 (2009).
- 3. J. D. Schnittman. Spin-Orbit Resonance and the Evolution of Compact Binary Systems. *Phys. Rev. D* 70, 124020 (2004).
- 4. L. Blanchet. Gravitational Radiation from Post-Newtonian Sources and Inspiralling Compact Binaries. *Living Reviews in Relativity* 5, 3 (2002).
- 5. M. Kesden, U. Sperhake, and E. Berti. Relativistic suppression of black hole recoils. *Phys. Rev. D* 81, 084054 (2010).

Acknowledgments

I would like to acknowledge most of all Emanuele Berti for the help received to develop this work. I thank Mike Kesden, Ulrich Sperhake, Giuseppe Lodato, Richard O’Shaughnessy, Marc Favata and Parameswaran Ajith for helpful discussions, as well as Yanbei Chen, Kennet Libbrecht and Alan Weinstein for the coordination of my research program. This work was supported by the NSF and the LIGO SURF program at the California Institute of Technology.





GENERAL DYNAMICS
Electric Boat

Get your career underway

The Nuclear Submarine Has Long been the silent backbone of United States Naval Supremacy.
ELECTRIC BOAT designs and builds these incredible machines.

We are looking for energetic and innovative individuals to continue the tradition of excellence that has become synonymous with **ELECTRIC BOAT**. We will show you how to apply your skills to the art of nuclear submarine design, engineering and construction.

ELECTRIC BOAT has immediate openings in Groton, Connecticut, for entry level engineers with zero to three years experience.

ELECTRIC BOAT is looking for engineering candidates with a minimum of a Bachelors degree in:

- Aerospace • Chemical • Civil • Computer
- Computer Science • Electrical • Mechanical
- Marine/Ocean • Naval Architecture

ELECTRIC BOAT offers an excellent salary and benefits package, including Tuition Reimbursement, Relocation assistance, and an excellent 401K Plan.

GENERAL DYNAMICS
Electric Boat

75 Eastern Point Road
Groton, CT 06340-4989

Please visit www.gdeb.com/employment
for more information, or contact
Electric Boat Employment office at 1-888-231-9662

US Citizenship Required Equal Opportunity / Affirmative Action Employer





Research and Development of External Occulter Technology for the Direct Observation of Extrasolar Planetary Systems : JPL Starshades Project

Author: Herbert Franz Mehnert Stadeler

Hometown: Mexico City, Mexico

College: MIT

Major: Aerospace Engineering

Year: Class of 2015

Hobbies: Working on cars, woodworking projects, robots, and design; astronomy

Mentors: Stuart Shaklan (JPL), Jeremy Kasdin (Princeton), and Peter Lawson (JPL)

**As**

www.curj.caltech.edu

28



Introduction

A Starshade Occulter is an optical structure approximately 30 meters in diameter. When deployed in an orbit around the Earth, it suppresses light from a target star by casting a shadow onto the image plane of a space telescope. A Starshade uses diffraction, scattering, and negative interference between waves to negate nearly all on-axis light in a telescope's image. This gives the image a very high contrast and allows for the observation of exoplanets orbiting a target star.

Under the Technology Development for Exoplanet Missions initiative created by NASA, our group assembled and tested the components of four Starshade Occulter petals. The process followed a set of steps including component alignment,

bonding, optical testing, structure assembly, material testing, and deployment testing.

In future missions, Starshades will allow for the direct observation of reflected light from Earth-like exoplanets. This will provide a powerful tool for the detection of exoplanets, as well as the capability to analyze the spectra of their reflected light. This spectral information is closely tied to the atmospheric properties of an observed planet, allowing us to search for the key components necessary for life.



Figure 1

Starshade Operation Diagram. A Starshade works in conjunction with a space telescope to image the light from a planet orbiting a distant star. The light from any object beyond the inner working angle reaches the telescope, but the light from everything within the IWA (notably the target star) is negated by the Starshade.

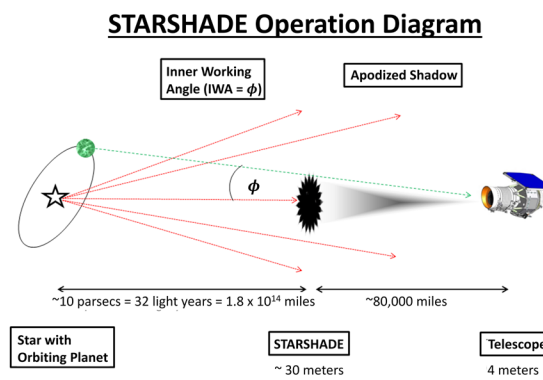
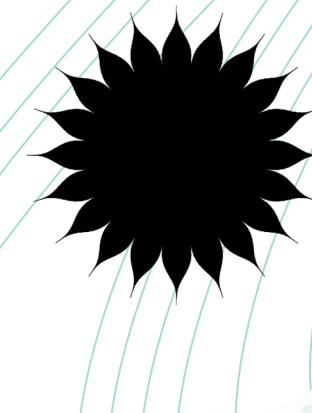


Figure 2

Profile of a 20-Petal Starshade. Diagram sourced from paper authored by Eric Cady, "Designing asymmetric and branched petals for planet-finding occulters." Credit to Jet Propulsion Laboratory.



II. Optical Design Considerations

The occulter works by casting a shadow onto the image plane of a space telescope in a very precise area, on-axis between the telescope, occulter, and star (see Fig. 1). We can predict the diffraction pattern caused by a plane wave originating at our target star interacting with our occulter using Babinet's principle. This principle tells us that the diffraction pattern of an opaque occulter of a particular shape will have an inverted diffraction pattern from that of an aperture of the same shape. If ray tracing and geometric optics explained the interaction between light and our structure fully, we would require only a disk of a particular size at a set distance to cast our shadow. However, the plane-wave interaction causes wave front propagation of infinitely many points on the optical edge, which scatters light into our image and creates bright spots in the shadow we hoped to create.

To resolve this issue, we approximate a smoothly apodized and infinitely extending transmissive gradient disk (which would provide

perfect shading in our image) with a binary petal system. Each petal has a profile determined by optical requirements to apodize the output function of the light-occulter interaction. The approximation improves as the number of petals in the Starshade increases, creating a better shadow. One such petal profile used in a Starshade Occulter is shown in Fig. 2. The apodization considerations, as well as a precisely shaped edge that controls the scattering off the petal boundary, allow light from a star to be suppressed while permitting light from objects around the star to enter the image plane.



Figure 3

Physical layout of Starshade Petal structure. Diagram sourced from recent Occulter Milestone final report, "Advancing Technology For Starlight Suppression Via External Occulter." Credit to Jet Propulsion Laboratory.

ADVANCING TECHNOLOGY FOR STARLIGHT SUPPRESSION VIA AN EXTERNAL OCCULTER

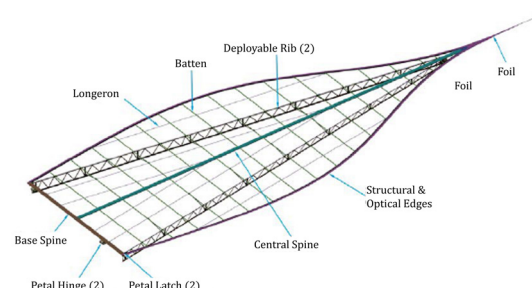
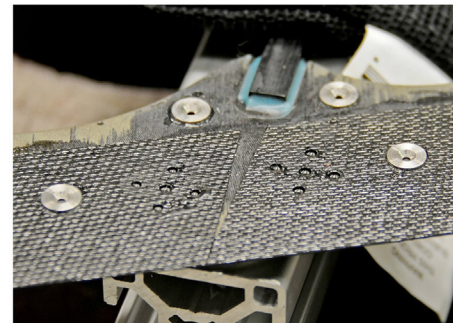


Figure 4

Close-up of an aluminum Starshade structural edge bearing a carbon Starshade optical edge. The edge resting on the piece of 80/20 aluminum extrusion is shaped precisely to follow a particular petal curve, allowing for successful apodization of target starlight. The carbon optical edge is also precisely shaped to control the diffraction of light off its boundary.



III. Petal Structure

The mechanical structure supporting the optical-edge used for precise starlight suppression is shown in Fig. 3, with battens, longerons, spines, hinges, ribs, and tip foil displayed. The petal components were machined from three main materials: a carbon-composite extrusion, high density foam, and aluminum sheet. The battens and longerons, made from carbon extrusion, make up the interacting components of the truss structure within the outside edge of each petal. The battens contain specific slots cut into the square extrusion that allow the longerons to thread through them.

High density foam was used to form the thick center-spine and base-spine of each petal, with aluminum making up the face-sheets. The longerons are threaded through battens placed perpendicularly to the central-spine and are embedded into the spine itself. The interaction between the spine, battens, and longerons gives the petal structure resistance to shear forces, as

well as a spring-like restoring force that is used during deployment to unfurl the petal.

The petal edge shown in Fig. 4, composed of a precisely shaped carbon optical edge attached to the aluminum structural edge, is bonded into slots cut in the side of the battens. The specific lengths of the battens define the petal profile. The structural edges serve to keep the battens in plane, provide rigidity to the structure, and support the optical edges that precisely follow the petal profile.

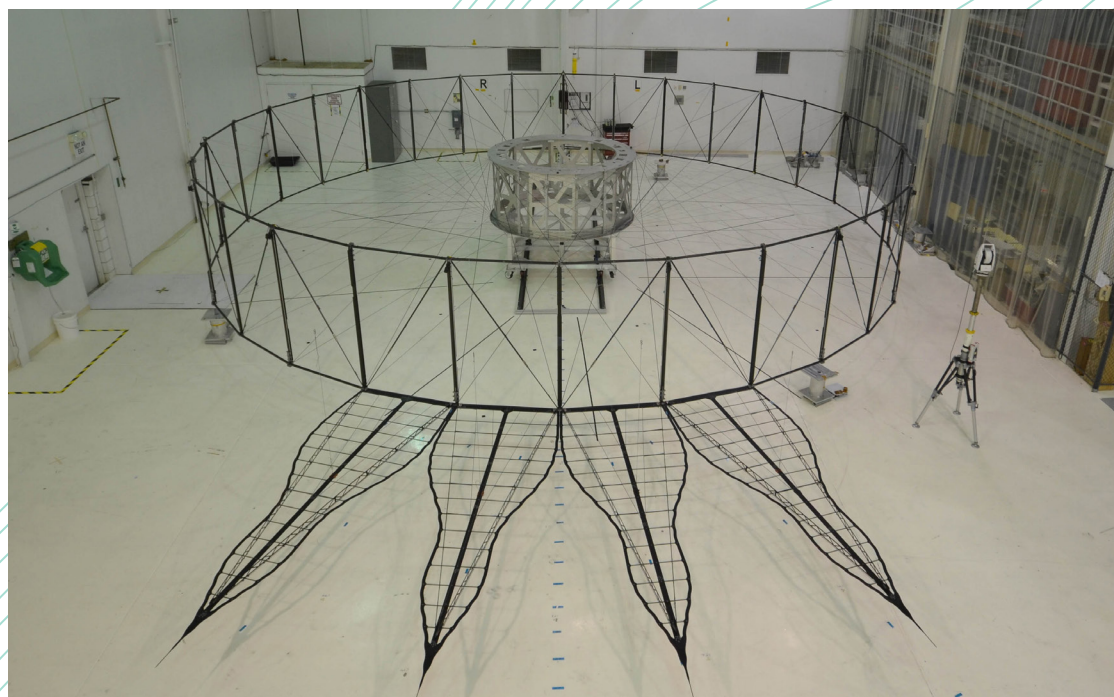
The final large components of the petals are the aluminum ribs, which provide rigidity to the structure out of plane. The ribs are connected to the main longeron through a series of rotating hinges, and to each adjacent longeron with springs contained inside pop-up tubes. As the petal unfurls from stow position around the central hub during deployment, these springs pop the ribs into place by rotating them from a parallel to a perpendicular orientation with respect to the petal face.



“The apodization considerations, as well as a precisely shaped edge that controls the scattering off the petal boundary, allow light from a star to be suppressed while permitting light from objects around the star to enter the image plane.”

Figure 5

Deployed petals on Starshade truss. The figure shows the central hub, truss, and petals, as well as the outriggers that fix the petal in place after deployment. Image taken during deployment testing at Northrop Grumman in Santa Barbara, California, 2013.





IV. Alignment and Assembly Processes

The assembly of the structure required high precision in a few instances, calling for precise alignment techniques. The most sensitive component to misalignment was the main longeron. As the pivot for the rib's piano hinge, it needed to be precisely placed in the corresponding batten slots to make the pivot axis straight enough for smooth deployment. This alignment was performed using a jig transit tool. The jig transit projected our line along the slots, which we measured and adjusted using the optics of the tool. Once a straight line through all slots was identified, we placed stops precisely along the length of the line to reference the longeron position. After the longerons were

constrained to their lines through the battens, they were epoxied in place. The assembled product is shown in Fig. 5.

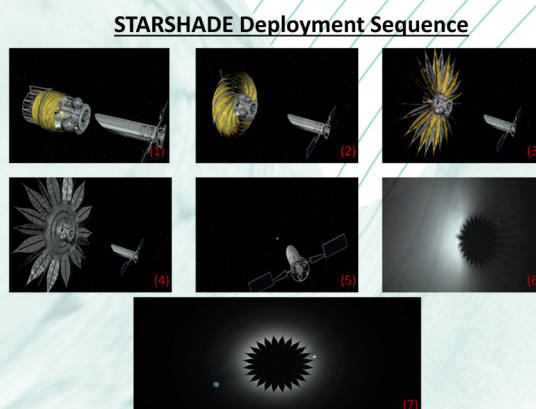
The other specific alignment requirement is the optical edge. Previously, this placement had been done by referencing positions from specific guide points along the structure using a FARO arm measuring system. Since our tests were on the structural and mechanical properties of the Starshade, our petals did not carry an optical edge. However, they would require alignment of their optical edges aligned using a FARO arm or similar system.



"Over a mission time span of two years, tens to hundreds of exoplanets could be discovered, and the first Earth-like planet capable of harboring life may be identified."

Figure 6

Starshade Deployment Sequence. The figure shows several key moments in the deployment, alignment, and use of a Starshade with a telescope. Panels 1 through 4 show the deployment of the Starshade from the stowed configuration to the operational configuration – the main focus of this research. Panels 5 through 7 show a conceptual representation of how the Starshade would operate.



NASA JPL – Starshades Project – 2013

V. Deployment

The stowing and deployment mechanism is needed to reduce the size of the launch package for a mission. Once deployed at the correct position relative to the mission telescope and the points of observation, the Starshade acts as a passive structure and does not stow or deploy its petals again. When the Starshade is stowed, the petals curl not only around the central hub, but around each other. This greatly decreases the diameter of the structure and allows everything to fit inside one rocket fairing for launch.

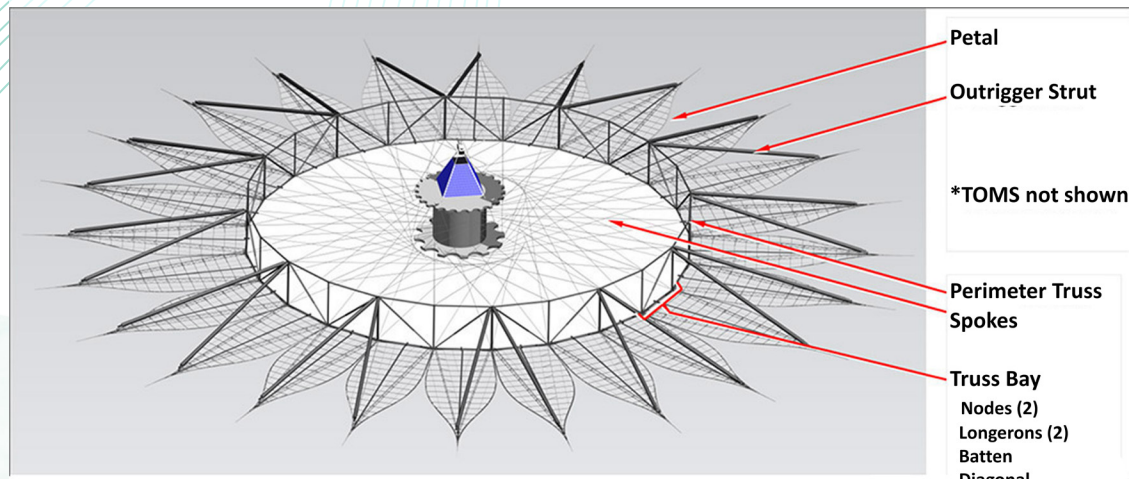
Fig. 6 outlines the deployment sequence. The petal structure is stowed by curling around a cylindrical hub parallel to the face of the petal.

Once released from this position, the restoring force in the curled spine and longerons begins to unfurl the petal. Shortly afterwards, springs pull the ribs into a perpendicular orientation with respect to the petal face. Next, the truss to which the petals are attached begins to expand, rotating the petals about their central spines and eventually locking them in an open-face position. Fig. 7 shows the shape of the Starshade after the truss has expanded and rotated the petals into place.



Figure 7

Diagram showing the deployed shape of a Starshade with 24 petals. Diagram sourced from recent Occulter Milestone final report, "Advancing Technology For Starlight Suppression Via External Occulter." Credit to Jet Propulsion Laboratory.



VI. What's Next?

The future application of this technology is a mission involving either an existing space telescope, or a purpose-built telescope named THEIA (Telescope for Habitable Exoplanets and Interstellar/Intergalactic Astronomy). The mission would require aligning a telescope with a Starshade at a distance of approximately 50,000 kilometers, and aligning both the telescope and the Starshade with a target star to be observed. Over a mission time span of two years, tens to hundreds of exoplanets could be discovered, and the first Earth-like planet capable of harboring life may be identified.

Before such a mission can be approved and

conducted, many technology and concept demonstrations must be completed. Our group's contribution to the second technology demonstration of Starshades will be followed by the third demonstration, which will consist of a full-scale test model developed on Earth.

Occulters have emerged as a promising technology for exoplanet research over the next several years, and expectations are high for the discoveries yet to come.



VII. Acknowledgements

Our group would like to acknowledge Dr. Stuart Shaklan, Dr. Jeremy Kasdin, and Dr. Peter Lawson for their contributions to not only this paper but to the Starshades project as a whole. We additionally acknowledge researchers such as Eric Cady for helping to establish the scientific knowledge base we have drawn from. Our group also acknowledges the mentors and JPL engineers who contributed to our project, including David R. Webb, Phil Walkemeyer, Vinh Bach, Eric Oakes, and Mark Thompson. This research was conducted at the NASA Jet Propulsion Laboratory, and was sponsored by NASA and by the Caltech Student Internship Program.

VIII. Further Reading

Kasdin, N. "Starshades for Exoplanet Imaging and Characterization: Key Technology Development." exep.jpl.nasa.gov. 2009.

Kasdin, N. "Verifying Deployment Tolerances of an External Occulter for Starlight Suppression." exep.jpl.nasa.gov. 2010.



IDA | FOR THE FUTURE

Integrity Based Objective Analyses

U.S. Citizenship Required www.ida.org

321567+94354965467
654964313210303467
973210313.10325420
654687603216763065
976410313475204756
7894231050.3657978
647689710.01354034
1321654987321065670
3874249732 16549248
754197319754812389

TIBCO™ www.tibco.com

Big Data

Analytics

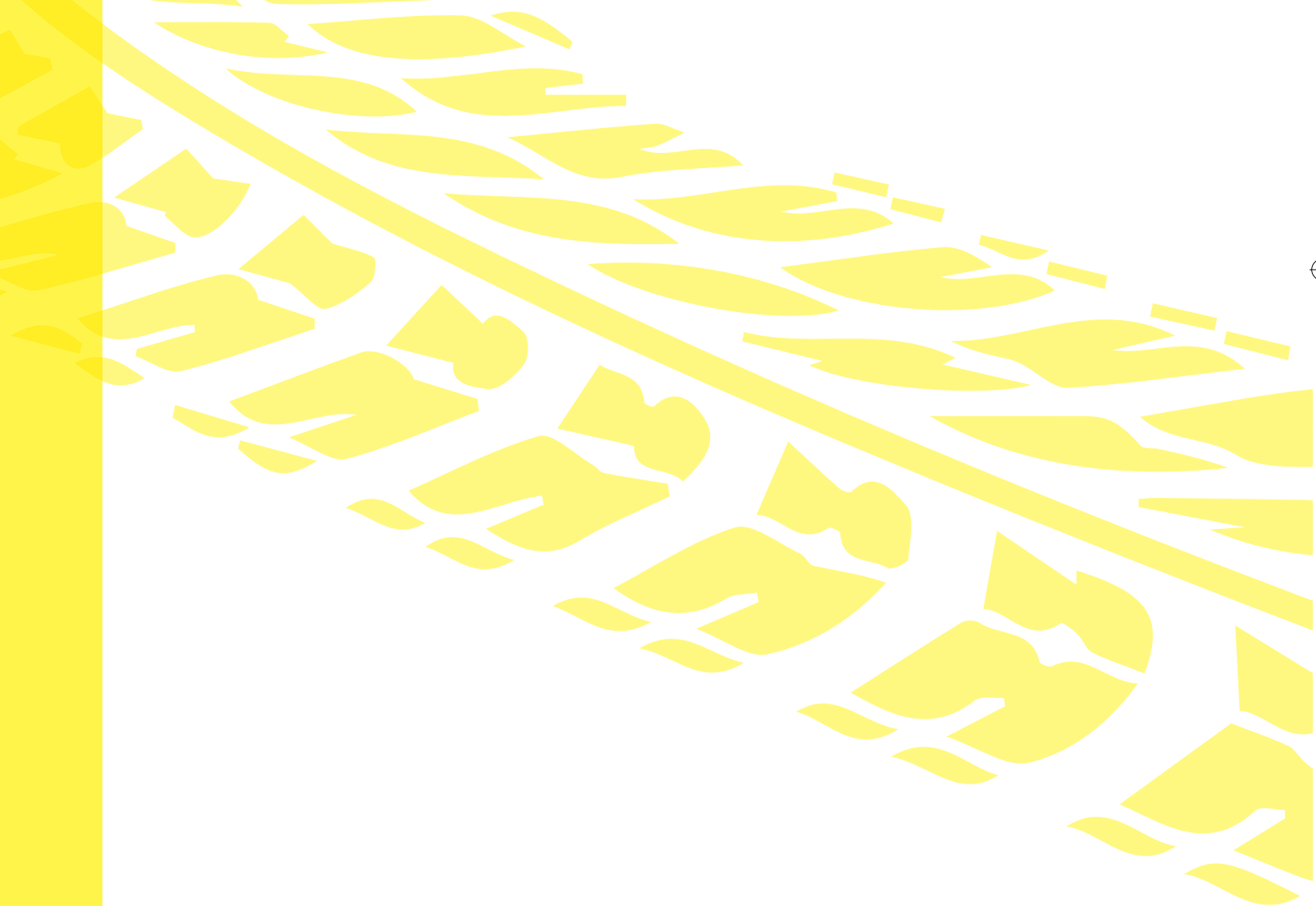
Real-Time Cloud

Data Mining

Mobile



Developing Force Models for Full Body Contact and Soft Tire-Solid Ground Interaction





Me

www.curj.caltech.edu

38



Author: Adam Ryason

Hometown: Carmel, NY

College: Rensselaer Polytechnic Institute

Major: Mechanical Engineering

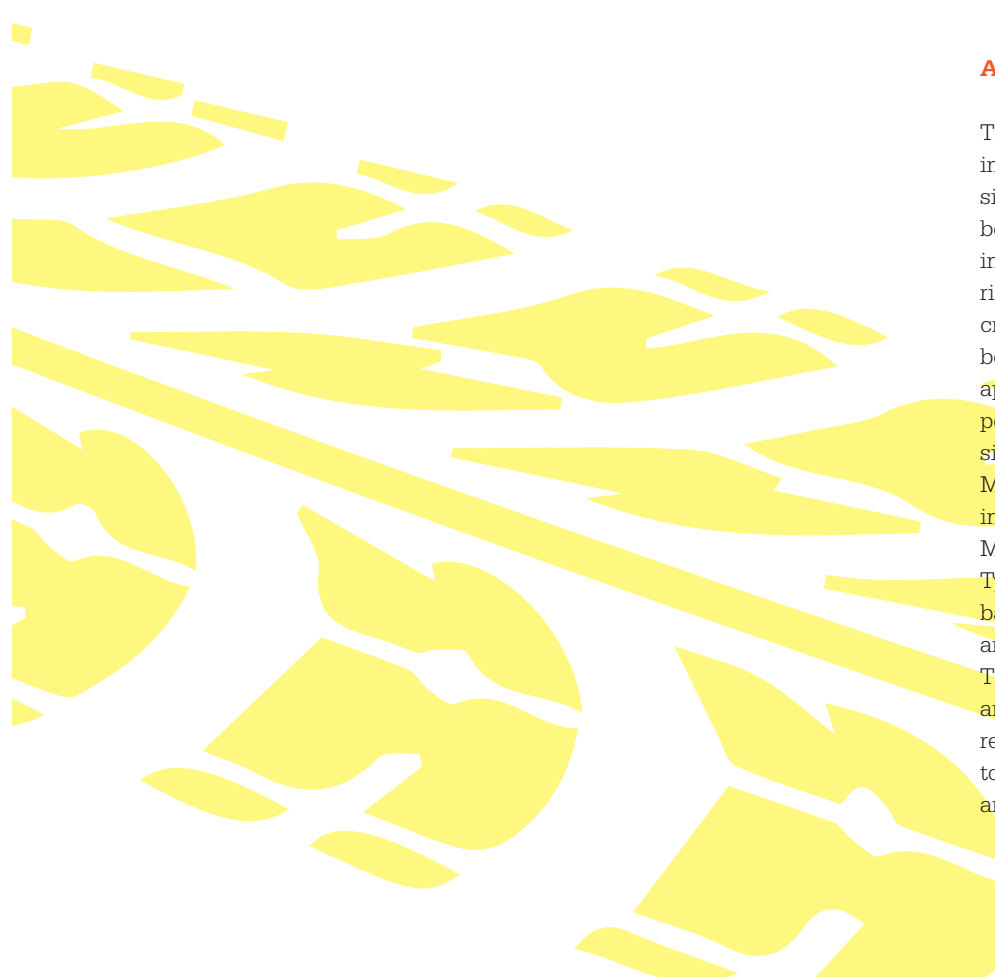
Year: Class of 2014

Hobbies: Watching movies, skiing, being with friends and family

Mentors: Abhinandan Jain (JPL) and Calvin Kuo (JPL)

Abstract

This research develops force contact models to be implemented and used in real-time dynamic simulations. There currently exists a need for full body contact modeling and soft tire on solid ground interaction. The Collision Forces model enables rigid bodies to interact with external objects by creating collision constraints between intersecting bodies and by using a penalty method that involves applying a spring-damper force based on the penetration distance. The Tyre Collision model simulates vehicle applied forces using the Pacejka Magic Formula, creating soft tire on solid ground interactions, which is favorable for High-Mobility Multipurpose Wheeled Vehicle (HMMWV). The Tyre Collision applies longitudinal and lateral forces based on the vertical load, camber angle, and slip angle while avoiding divergence at low velocities. The contact models are applied to a bipedal robot and rover vehicles assembly for testing. Various regression tests are performed and a GUI was used to ensure that the simulations respond naturally and results are compared to known methods.





I. Introduction

Previous contact models for tires in simulations developed in the Dynamic and Real-Time Simulations Lab (DARTS) have always been approximations that no longer suffice when it comes to large collisions or soft terrain. In the past simulations, contact pads were placed on the ends of bodies to apply point forces onto systems. This method of force application is used when the surface that the force acts on is small, or when rigid body motions need to be simplified. In contrast, full-body contact models allow forces to be distributed across an area by creating nodes where contact is made; they can be described by solving the dynamics for the set of nodes. The dynamics can be better represented for collisions or large contact area surfaces that have forces distributed across the body through application of

a full-body contact model to a rigid body. In another area of contact models, tires have regularly been modeled as rigid bodies that do not deform. The previous models can be used to properly represent hard-tires on hard ground; however, as the tire and ground become softer, the tire behaves more like a deformable body. As a result, rigid body dynamics are not accurate when used to describe deformable bodies. There is currently a need to model tires in sand-like terrain, so a soft-tire model is desired. The Pacejka Magic Formula (MF) is a semi-empirical method for deformable tires that uses coefficients for various tire models that will return the horizontal force for a deformed tire.



Me

www.curj.caltech.edu

40

"The TCM was successfully implemented into the rover and HMMWV simulations, where they each were capable of settling, accelerating, stopping and turning on flat terrain."

II. Behind the Scenes

The DARTS lab develops several multi-mission space system simulation tools for closed-loop development and testing of algorithms and software. The software developed has been applied to entry, descent and landing, flight and ground-vehicle simulations. Research is also conducted on multi-body dynamics, to be developed and implemented into existing contact models.

Contact models are used to calculate forces for simulations using dynamic equations appropriate for a system. These forces are then used to calculate the acceleration of the bodies using Newton's Second Law. Through integrating the accelerations and applying boundary conditions based on the initial orientation, the velocity and displacement are determined and the dynamics for the system are applied.

The integration is performed using the Runge-Kutta (RK4) method. RK4 is an iterative method for computationally approximating integrals. The approximation is calculated by adding the initial value to a weighted average of the slope of four subsequent steps multiplied by the step size. The RK4 method is a fourth order method, producing total accumulated error of order four. The integrator within the models uses CVODE, a 3rd-party software that permits adaptive integration to take steps based on errors from an initial step size. Smaller step sizes will be used on steep functions in which more time is required to obtain results; larger step sizes can be used for smoother functions without losing precision.



III. A TALE OF TWO MODELS

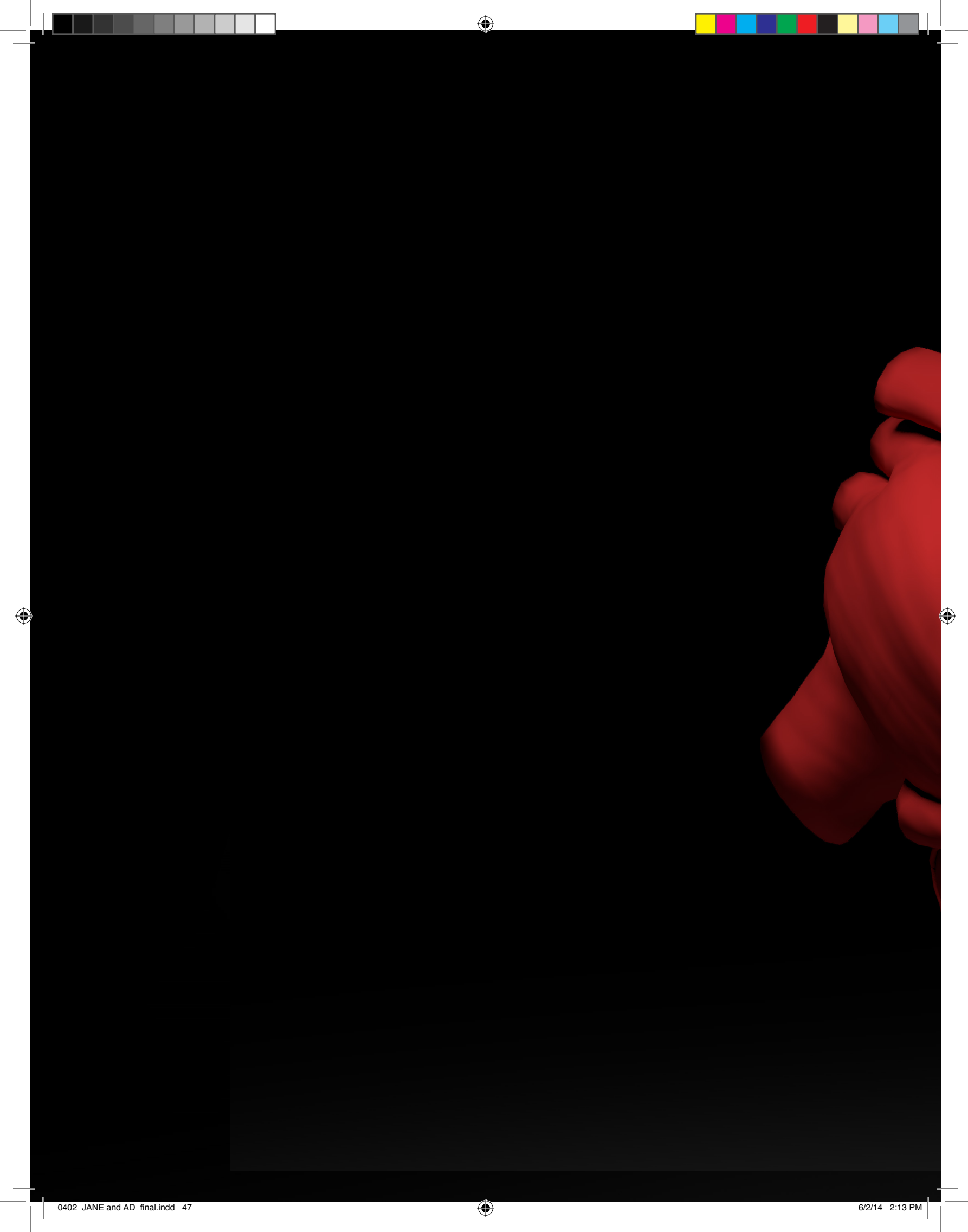
“The CFM behaved as expected by generating the nodes and yielding collision forces for a solid rigid body when the actuators were prescribed and limited testing was done on the Atlas as a multibody system.”

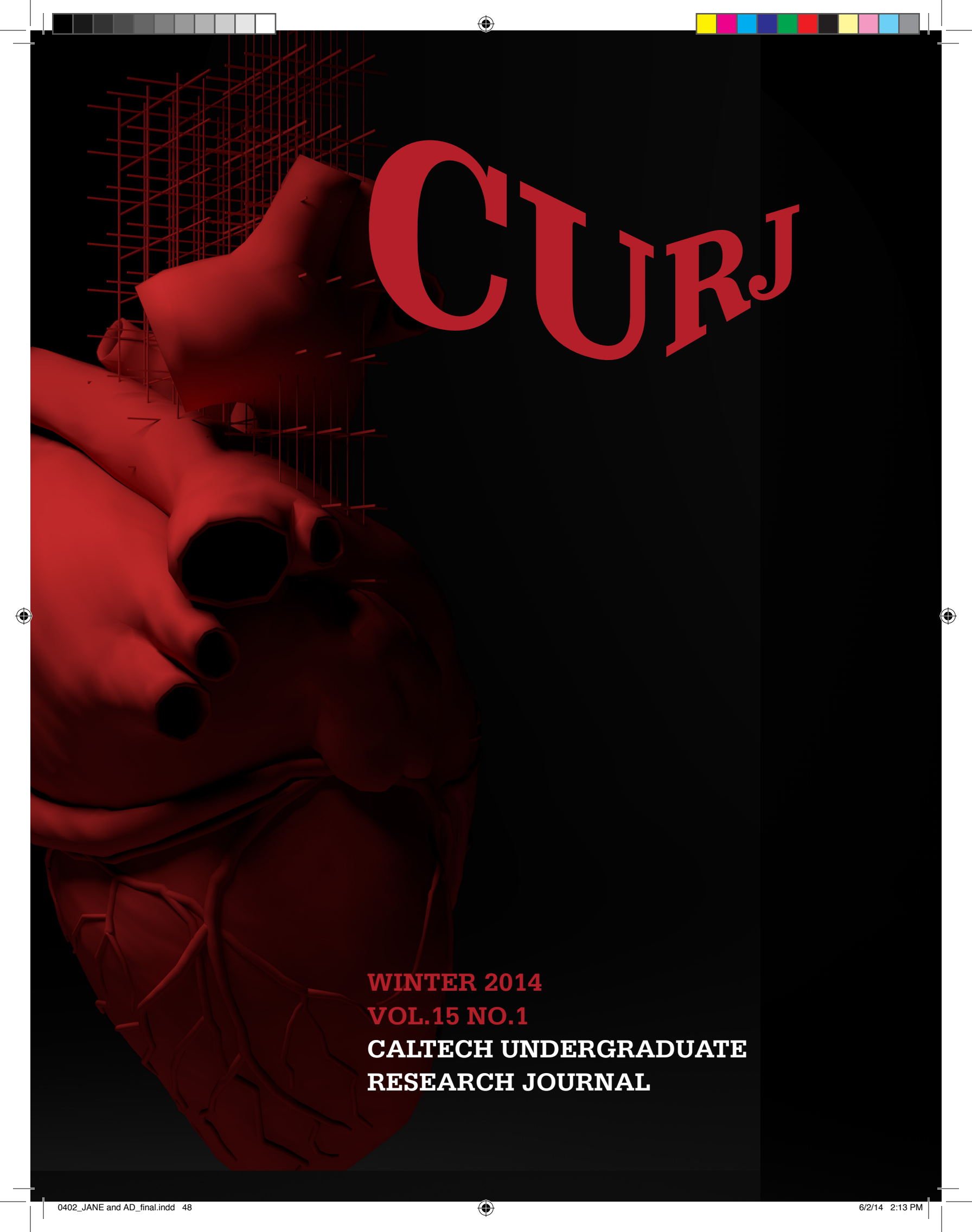
III.1 Collision Forces Model

The Collision Force Model (CFM) is developed to apply full-body contact forces in collisions or large surface area contacts. When contact is detected in the DARTS Shell, the model creates a constraint node pair between the two bodies where one node lies on the first body and the other node is on the second body. The penetration displacement is then retrieved from the DARTS shell and input into a penalty method algorithm that returns the force to apply to the node based on a spring-damper system.

The CFM was applied to a bi-pedal robot simulation that represented an Atlas for testing. The actuator joints on the robot were initially

locked to simplify the simulation so that the robot was a single rigid body. Various simulations were conducted in which the Atlas freefell in a standing position and collided with the ground. Static simulations where the Atlas lay or stood in various orientations were also conducted. The terrain stiffness, frictional, and damping coefficients were tuned to properly simulate a ground terrain and make collisions more realistic. To simplify debugging the simulation, a GUI was used to show normal vectors to collisions and the force vectors associated with them.





CURJ

**WINTER 2014
VOL. 15 NO. 1
CALTECH UNDERGRADUATE
RESEARCH JOURNAL**

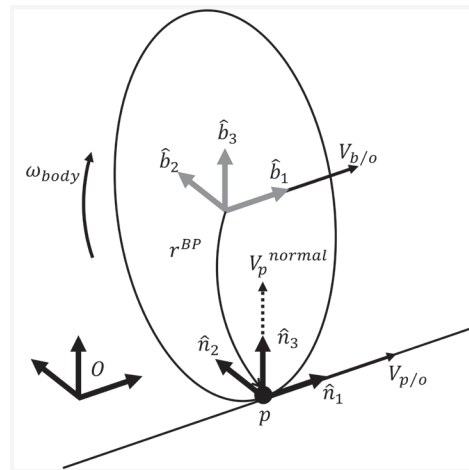


Figure 1

Calculating the normal velocity.

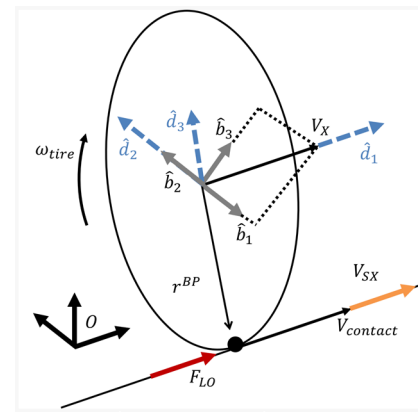


Figure 2

Calculating the slip coefficient.

III.2 Tyre Collision Model

The Tyre Collision Model (TCM) is based off of Pacejka's Magic Formula (MF) to compute the forces acting horizontally on a soft-tire. Various tires are characterized by coefficients for each important force that it can produce at a contact patch. These coefficients are then used to generate equations that show how much force is generated for a given normal force. The MF has a general form:

$$\vec{f}_{x,y} = \vec{f}_z \cdot D \cdot \sin[C \cdot \tan^{-1}\{Bk - E(Bk - \tan^{-1}Bk)\}] \quad (1)$$

FZ is the normal force applied by the tire; k is the slip coefficient; and D, C, B and E are constants based off of empirical results (respectively peak value, shape factor, stiffness factor and curvature factor). The normal force is calculated using a spring-damper equation:

$$\vec{F}_z = k\vec{x}_{pen} + c\vec{v}_{norm} \quad (2)$$

x_{pen} is the penetration distance, and v_{norm} is the normal velocity.

As seen in Figure 1, the velocity of node p is determined by retrieving the linear and angular velocity of the contact node on the tire with respect to the inertial frame and calculating the absolute linear velocity of the contact node. The normal velocity is derived by projecting the node velocity onto the normal vector:

$$\vec{v}_p = V_{p/o} + \omega_{body} \times r^{BP} \quad (3)$$

$$\vec{v}_{norm} = \vec{v}_p \cdot \hat{n}_1 \quad (4)$$

The slip coefficient k is used for calculating the longitudinal force and it is a ratio of the slip velocity and absolute value of the hub velocity. As seen in figure 2, the slip velocity, VSX, is the difference between the hub velocity and the velocity of the contact point, V_p .

$$k = \frac{V_{SC}}{|V_x|} \quad (5)$$

$$V_{SC} = V_x - V_p \quad (6)$$

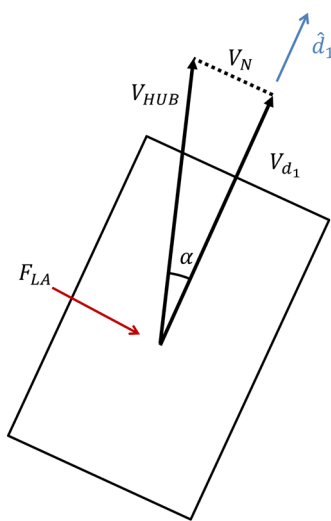


Figure 3

Calculating the latitudinal force.

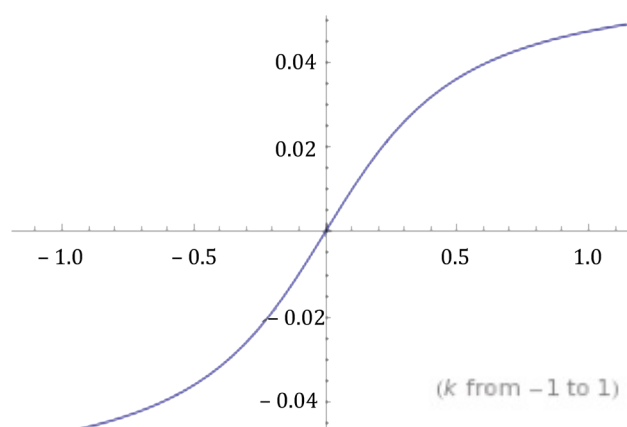


Figure 4

The corresponding MF curve for D = 1.154, C = 0.05, B = 1.75, E = 0.97. The y-axis is the normalized force and the x-axis is the coefficient, k.

Where both the hub and contact point velocity are along the direction vector:

$$V_x = \vec{V}_x \cdot \hat{d}_1 \quad (7)$$

$$V_p = \vec{V}_p \cdot \hat{d}_1 \quad (8)$$

The direction vector is determined from the cross product of the normal vector and the wheel axle, which is a geometric property:

$$\hat{d}_1 = \omega_{tire} \times \hat{n}_1 \quad (9)$$

To calculate the latitudinal force, the constant k is replaced with , where alpha is the angle between the velocity of the hub and the directional component of the velocity as seen in Figure 3. Using this coefficient in the MF results in a latitudinal force, F_{LA}:

$$\alpha = \text{atan}\left(\frac{V_N}{V_{d_1}}\right) \quad (10)$$

To adapt the MF to code, appropriate fitting constants (D, C, B, E) had to be selected. The initial values were selected based on typical road

conditions. The values were then tuned to fit the system that they were representing. The final values selected were D = 1.154, C = 0.05, B = 1.75, E = 0.97.

Thresholds were enforced to prevent divergence, specifically when the velocity was near zero and when the system was settling. In order for the horizontal forces to be calculated the hub absolute velocity had to be greater than .001 m/s. An algorithm checked the local slope of the normal force to determine whether the system had settled or not, and if the slope was greater than .01 N/s, then the horizontal forces were not calculated. The TCM was tested in a rover simulation and a High Multipurpose Wheeled Vehicle (HMMWV) where it accelerated, stopped, and performed varying heading changes. The simulations were viewed and compared to simulations using previous tire models. Tests were completed on flat terrain and terrain including obstructions and bumps.



Me

www.curj.caltech.edu

44

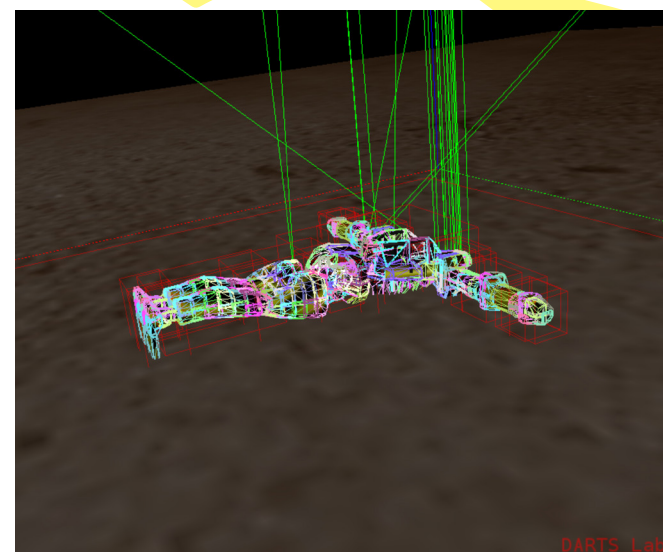


Figure 5

Normal vectors at contact nodes.

IV. Results

When the CFM was tested on Atlas, it properly produced contact constraint couples. When viewing the simulation with the contact normals turned on as seen in Figure 4, the Atlas was capable of settling and remaining at rest. The green lines in the figure are the normal vectors at the nodes that are created by the model file.

It was seen that certain body-terrain interactions did not produce sufficient nodes and may not have been recognized by the model. Specifically, when standing, the Atlas did not observe forces on itself until its ankle made contact with the ground. It seemed that the simulation was ignoring both feet. Problems occurred with plane geometry when a node fully breaks through, causing forces to disappear. This was fixed by switching the plane terrain to a block such that if a

node breaks through the plane completely forces will always be applied.

The TCM was successfully implemented into the rover and HMMWV simulations, where they each were capable of settling, accelerating, stopping and turning on flat terrain. Turns were completed up to and including 20 degrees per second, and this involved left- and right-handed turns as well as sequential figure eights. After each turn, the car reached its starting point with a heading of zero and only a displacement around a car width. Testing is to continue on abnormal terrain and performing normal car motions such as lane changes.



V. Discussion

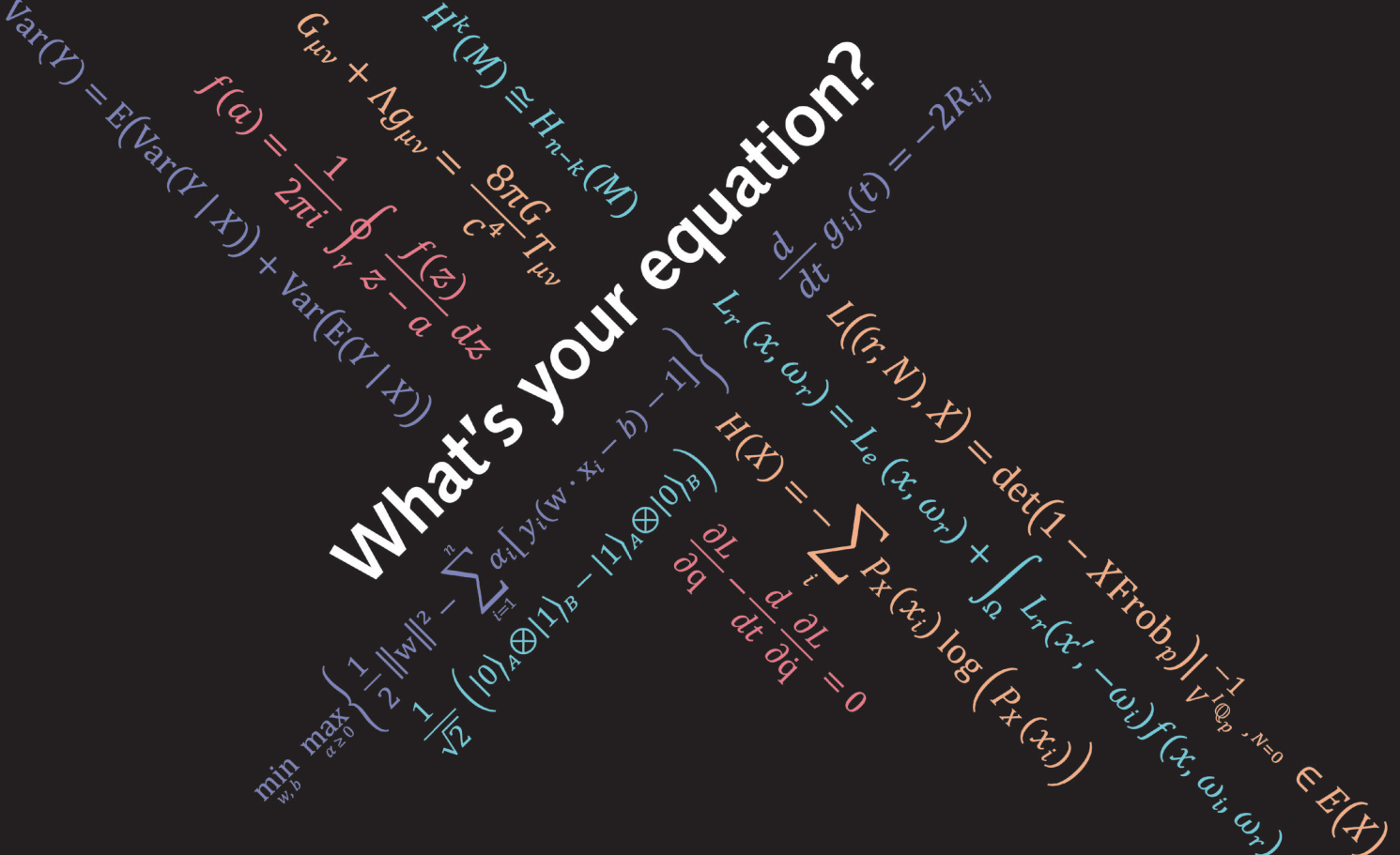
The CFM behaved as expected by generating the nodes and yielding collision forces for a solid rigid body when the actuators were prescribed and limited testing was done on the Atlas as a multi-body system. The Atlas model itself needs to be looked into because as stated in the results, some bodies were not creating collision constraint nodes like they should have been. Future work would be to apply feed forward control to the simulations to ensure that model works in that field as well.

For the TCM, the main problem came from thrashing, where the integrator does not converge on a solution. Inappropriate constants caused the simulation to have step size errors where the step size became infinitesimally small due to errors in the computation. The original slope of the MF curve was too high, requiring an

extremely small step size in order to converge into a value. The slope of the MF curve is mostly influenced by the product of constants B, C and D. The shape factor C affects mostly the slope of the curve; when it is lowered, the integration can occur in greater steps and eliminate the thrashing taking place. The thresholds were also very important to the integration of the model. Before they were implemented, simulations had run into many step size errors when the normal force was settling. Future work will consist of applying this contact model on other ground vehicle simulations and projects. More work can be completed to choose better fitting constants to optimize the calculated forces and step size.

References

- [1] Pacejka, A. B.(2006). The Magic Formula Tire Model Tire and Vehicle Dynamics
- [2] J. Cameron, C. Kuo, A. Jain, H. Grip Real-Time and High-Fidelity Simulation Environment for Autonomous Ground Vehicle Dynamics 2013 NDIA Ground Vehicle Systems Engineering and Technology Symposium
- [3] C. Lim, A. Jain (2009). "Dshell++: A Component Based, Reusable Space System Simulation Framework" Third IEEE International Conference on Space Mission Challenges for Information Technology(SMC-IT 2009)
- [4] A. Jain, J. Guineau, C. Lim, W. Lincoln, M. Pomerantz, G. Sohl, R. Steele "Roams: Planetary Surface Rover Simulation Environment", International Symposium on Artificial Intelligence, Robotics and Automation in Space (i-SAIRAS 2003), (Nara, Japan), May 19-23 2003



Independent variables welcome.

The D. E. Shaw group is an investment and technology development firm with an international reputation and a decidedly different approach to doing business.

Combining insights from quantitative fields, software development, and finance, we're widely recognized as a pioneer in computational finance. And yet our culture doesn't fit the typical corporate mold: though we're competitive people, we're not competitive with each other; our grassroots philanthropic initiatives are one of the many ways we stay involved in the community; and we value the environment that continually allows us to learn from our colleagues.

The firm is currently looking for quantitative analysts, software developers, traders, information technologists, finance associates, and rotational

associates. We're looking for rigorously analytical idea generators to join our team, but consider yourself warned: new hires contribute to the business from day one.

Stop by our booth at the Caltech Career Fair to learn more about opportunities offered at the D. E. Shaw group.

Realize your potential. www.deshaw.com

Members of the D. E. Shaw group do not discriminate in employment matters on the basis of race, color, religion, gender, pregnancy, national origin, age, military service eligibility, veteran status, sexual orientation, marital status, disability, or any other protected class.

DE Shaw & Co